
6th International Conference on
Case Histories in Geotechnical Engineering, Arlington, VA, August 11-16, 2008

Ground Vibrations Induced by Impact Pile Driving

K. Rainer Massarsch
Vibisol International AB
Ferievägen 25, S-161 51 Bromma, Sweden
E-mail: <rainer.massarsch@geo.se>

Bengt H. Fellenius
Bengt Fellenius Consultants Inc.
1905 Alexander St. SE, Calgary, AB, T2G 4J3
E-mail : <Bengt@Fellenius.net>

ABSTRACT

The importance of vibration problems induced by pile driving is addressed and guidelines for establishing limiting vibration levels with respect to buildings with different foundation conditions are presented. Basic concepts of pile dynamics and stress-wave measurements, which were developed for the determination of driving resistance and bearing capacity of impact-driven piles, provide important information about ground vibration induced by pile penetration. Dynamic hammer properties and geometry as well as the driving process are important for ground vibration emission from the pile. It is shown that the energy-based, empirical approach, which is still widely used by practicing engineers, is too crude for reliable analysis of ground vibrations and can even be misleading. The main limitations of the energy approach are the assumption that driving energy governs ground vibrations, the omission of geotechnical conditions and soil resistance, and the uncertainty with regard to input values.

Three types of ground waves are considered when analyzing pile driving: spherical waves emitted from the pile toe, cylindrical waves propagating laterally from the pile shaft, and surface waves, which are generated by wave refraction at the ground surface at a critical distance from the pile. These three wave types depend on the velocity-dependent soil resistance at the pile-soil interface. The most important factor for analyzing ground vibrations is the impedance of each system component, i.e., the pile hammer, the pile, and the soil along the shaft and at the pile toe. Guidance based on geotechnical conditions is given as to the selection of appropriate impedance values for different soil types.

A theoretical concept is presented, based on a simplified model that considers the strain-softening effect on wave velocity in the soil, making it possible to calculate the attenuation of spherical and surface waves and of cylindrical waves generated at the pile toe and the pile shaft, respectively. The concept is applied to define *k*-values, which have been used in empirically developed models and correlated to type of wave and soil properties.

An important aspect of the proposed prediction model is the introduction of vibration transmission efficacy, a factor which limits the amount of vibration force that can be transmitted along the pile-soil interface (toe and shaft). Results from detailed vibration measurements are compared to values calculated from the proposed model. The agreement is very good and suggests that the new model captures the important aspects of ground vibration during penetration of the pile into different soil layers. Finally, based on the presented model, factors influencing the emission of ground vibrations during impact pile driving are discussed.

INTRODUCTION

Pile driving is an age-tested method of constructing foundations where adequate ground support is not directly available. However, it is also a source of negative environmental effects. Noise and air pollution are the most commonly expressed concerns, but they are also relatively easily alleviated. In contrast, vibrations originating from the impact driven pile are both difficult to determine beforehand and costly to mitigate, while potentially having serious adverse effect on adjacent structures and their foundations, as well as on vibration-sensitive installations and occupants of buildings. Not having confidence in how to assess the risk of ground vibrations during pile driving, regulatory authorities often feel compelled to impose restriction on the use of driven piles and sheet piles or to choose alternative foundation solutions.

At present, and in contrast to other aspects of pile dynamics, the calculation of ground vibrations is still based on crude empirical rules developed about 30 years ago. For example, while energy-based relations for calculating pile bearing capacity (so-called dynamic formulae) have been discarded due to their lack of sound theoretical base and, therefore, inherent inaccuracy, the concept is still being used to predict ground vibrations due to pile driving. For either application, however, energy-based methods are irrational and neglect fundamental aspects of dynamic pile-soil interaction (Goble et al., 1980; Hope and Hiller, 2000; Martin 1980; Massarsch 1992 and 2005; Selby 1991). On the other hand, without an understanding of the fundamental aspects of hammer-pile-soil interaction, it is difficult even with sophisticated numerical methods to model the dynamic pile penetration and to predict ground vibrations. Surprisingly few publications have

addressed in a scientific way vibrations due to pile driving as a dynamic pile-soil interaction problem. Most published case records suffer from lack of basic information regarding the equipment and method of pile driving, dynamic properties of the pile and the surrounding soil or details about the vibration response obtainable from dynamic measurements. Geotechnical information is often insufficient and has resulted in difficulties to interpret results of case histories and to advance empirically developed prediction models.

The current reliance on empirical models puts the construction industry in a precarious situation in the light of recent rapid development of potentially powerful construction equipment for installing piles, such as hydraulic impact hammers and advanced vibratory driving equipment, when their use is restricted due to vibration concerns. The advancement of field measurements and electronic data acquisition systems has now made it possible to monitor and document not just pile penetration resistance and rate, but also the dynamic response of the ground and of adjacent structures. Sophisticated computer programs are available to the engineer, offering a variety of methods to analyze signals in the time and frequency domain. The main constraint at present is lack of understanding how to interpret results of vibration measurements. Significant progress has also been made with respect to determining dynamic soil parameters from seismic field and laboratory tests, which were developed primarily for earthquake and machine foundation applications, but could also be applied to the analysis of vibrations from pile driving.

In this paper, the authors discuss the most important aspects that govern the propagation of driving energy from the source of the vibrations — the pile driving hammer — to the surrounding soil layers. It is shown that current models result in crude predictions that ignore the influence of geotechnical site conditions and neglect the fact that the velocity-dependent resistance between the pile and the soil is the source of ground vibrations. This effect can be analyzed using concepts developed in dynamic pile analysis.

Based on a rational concept, the authors put forward a method for estimating vibrations from pile driving, which includes the force that is applied to the pile head, the dynamic stresses in the pile and the dynamic resistance along the pile toe and pile shaft. Emphasis is placed on the development of a prediction method applicable to engineering practice that incorporates essential aspects of the pile driving and wave propagation process, as well as geotechnical conditions. The proposed model is compared to field measurements from a well-documented case history. Finally, factors influencing ground vibrations during impact pile driving are discussed as well as measures to reduce ground vibrations.

RISK OF BUILDING DAMAGE

When planning a project, where driven piles or sheet piles are to be used, the design engineer must identify potentially vulnerable structures and installations in the vicinity of the project site and propose limiting values of ground vibrations. As part of this task, the risks must be assessed of vibration damage to structures and vibration-susceptible installations or environmental aspects affecting occupants of buildings. As the prediction of building damage can be complex, theoretical methods have low reliability. However, it is possible to assess the potential damage to buildings based on statistical observations. This approach is used in codes and standards but is limited to the specific conditions in the region where the observations were made. Therefore, local building standards should be applied with caution in other regions, where pile driving methods, geological conditions, and building standards may be different.

Swedish Standard for Pile Driving Vibrations

Several standards pertaining to ground vibrations from traffic and construction activities have been developed (Massarsch and Broms 1991). The Swedish Standard SS 02 542 11 (SIS 1999) is one of the more elaborate standards currently available. It deals with vibrations caused by piling, sheet piling but also includes soil compaction and provides guidance levels (limit values) for acceptable vibrations of buildings based on more than 30 years of practical experience in a wide range of Swedish soils. It is important to note that the vibration limit values apply to buildings at the foundation level and do not take into consideration psychological consequences (noise or comfort) for occupants of buildings. Neither do they consider the effects of vibrations on sensitive machinery or equipment in buildings. Although, the guidance levels given in the Swedish standard should be used with caution in areas with different geological conditions and building construction methods, they can provide useful information as to which factors should be taken into consideration when assessing the risk of building damage.

The guidance levels are based on experience from measured ground vibrations in terms of the vertical component of vibration velocity and observed damage to buildings with comparable foundation conditions. This is a severe limitation when considering the effect of horizontal vibrations on buildings founded on long piles, as piles provide little resistance to horizontal excitation. Moreover, the standard does not address the risk of liquefaction or densification of the soil (especially disregarding the risk for loose sand and silt), which can lead to unacceptable total or differential settlement of the structure.

The standard defines a vibration limit value, v, in terms of peak value of the vertical vibration velocity, which is taken to

be the maximum acceptable value. If this value is not exceeded, damage to buildings and their foundation is unlikely to occur. Vibrations should be measured at the building foundation level in the closest location from the piling site. Its value is modified according to range of soil types into which the piles are driven, building types, building materials, and foundation types, as expressed in Eq. 1.

$$v = v_0 F_b F_m F_g \quad (1)$$

where v = guidance level (vertical component) of vibration velocity (mm/s)
v_0 = vibration velocity based on soil type (mm/s)
F_b = Building Factor
F_m = Material Factor
F_g = Foundation Factor

Recommended values for v_0 are given in Table 1 for vibrations caused by pile driving in sedimentary soil, glacial till, and to bedrock, considering two cases: driving of piles and soil compaction. The values indicated for the latter work are often assigned to vibratory driving of piles and sheet piles.

Table 1. Vibration velocity for different soil types, v_0, mm/s

Soil Type	Piling, Sheet Piling, or Excavation	Compaction Work
Clay, silt, sand, or gravel	9	6
Glacial till	12	9
Bedrock	15	12

Swedish Standard SS 02 542 11 (SIS 1999)

The Building Factor, F_b, depends on the susceptibility of building with regard to vibrations separated on five classes as shown in Table 2. Classes 1 - 4 apply to structures in good condition. As suggested for Class 5, buildings in poor structural condition should be assigned a lower building factor.

The Material Factor, F_m, depends on vibration sensitivity of the structural material and is divided into four classes, as shown in Table 3. The most sensitive material component of the structure determines the class to be applied.

The Foundation Factor, F_g, separates between building on type of foundation, as shown in Table 4. Buildings on piled foundations are accorded higher factors due to their reduced sensitivity to ground vibrations in the vertical direction. However, if the horizontal vibration component is high, this limiting value should be adjusted, as pile-supported foundations has a low resistance to horizontal excitation. Also, the effect of vibrations on loose, granular soils is not considered in the standard, but such soils may be particularly susceptible to vibration-induced settlements (Massarsch, 2000).

Table 2. Building Factor, F_b

Class	Type of Structure	Building Factor
1	Heavy structures such as bridges, quay walls, defense structures etc.	1.70
2	Industrial or office buildings	1.20
3	Normal residential buildings	1.00
4	Especially susceptible buildings and buildings with high value or structural elements with wide spans, e.g., church or museum	0.65
5	Historic buildings in a sensitive state as well as certain sensitive ruins	0.50

Swedish Standard SS 02 542 11 (SIS 1999)

Table 3. Material Factor, F_m

Class	Type of Building Material	Building Factor
1	Reinforced concrete, steel, or wood	1.20
2	Unreinforced concrete, bricks, concrete blocks with voids, light-weight concrete elements, masonry	1.00
3	Light concrete blocks and plaster	0.75
4	Limestone	0.65

Swedish Standard SS 02 542 11 (SIS 1999)

Table 4. Foundation Factor, F_g

Class	Type of Foundation	Foundation Factor
1	Spread footings, raft foundations	0.60
2	Buildings founded on shaft-bearing piles	0.80
3	Buildings founded on toe-bearing piles	1.00

Swedish Standard SS 02 542 11 (SIS 1999)

Application Example

As an example on the use of the Swedish standard (SIS 1999), assume that piles are driven in clayey soils in the vicinity of a residential building (Building Factor, F_b: 1.0) with walls of light concrete blocks and plaster (Material Factor F_m: 0.75), and supported on shaft-bearing piles (Foundation Factor, F_g: 0.8). According to Table 1, the ground vibration velocity, v_0, to choose is 9 mm/s and the values inserted into Eq. 1 provide a maximum acceptable ("allowable") vertical vibration velocity, v, of 5.4 mm/s. Thus, in a risk analysis for this piling project, the design engineer should limit permissible building vibrations to 5.4 mm/s (to be measured in the vertical direction at the base of the building).

GROUND VIBRATIONS FROM IMPACT PILE DRIVING

Vibration Transmission Chain

This paper focuses on ground vibrations induced by impact pile driving and should not be applied without due modifications to vibratory driving of piles or sheet piles. For aspects of vibrations from vibratory pile driving, basic principles of the pile penetration process and ground vibrations, reference is made to Massarsch and Westerberg (1995) and Massarsch (2002). When the pile driving hammer impacts the pile head, a stress (or strain) wave, i.e., vibration, is created that propagates at certain frequencies and amplitudes down the pile, into the soil, and in under and into adjacent structures. The main aspects of vibration propagation during the driving of piles with an impact hammer consist of four main points as illustrated in Fig. 1. Unless the entire chain of vibration transmission is considered, it is not possible to appreciate fully the cause of ground vibration problem.

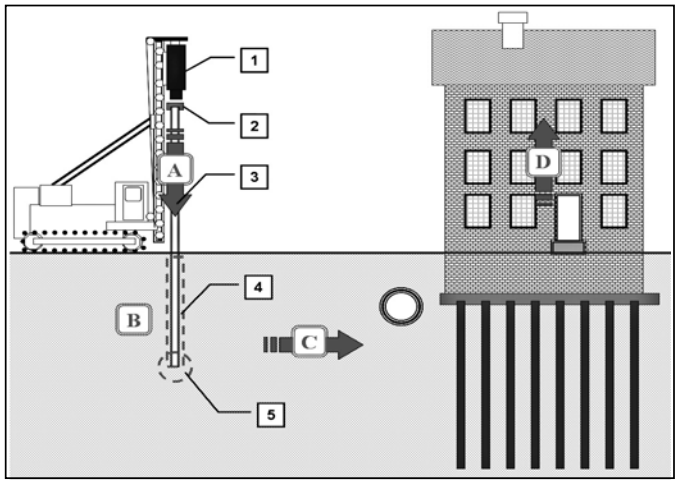

Fig. 1. Transfer of vibrations from the hammer, through the pile, into surrounding soil, under and into adjacent buildings (Massarsch 2005).

A. Wave propagation in the pile: energy generated by the impact of the hammer (1) at the pile cap and pile head (2) which is transmitted through the pile (3).

B. Pile-soil interaction: along the pile shaft (4) and at the pile toe (5).

C. Wave propagation in the ground: transmission of vibrations through soil layers and the groundwater.

D. Dynamic soil-structure interaction: dynamic response of foundations, vibration amplification in structures, and installations.

When assessing vibrations caused by pile driving, most investigations focus on the generation of energy by the impacting hammer (A) and the propagation of vibrations in the ground (C). In some cases, the soil-structure interaction and dynamic response of buildings subjected to vibrations (D) are addressed without considering the important aspect of transfer of stresses and vibrations through the entire system: including vibrations transmitted from the hammer to the pile and the dynamic properties of the soil (B), despite that this is the most important part in the vibration transmission chain.

Usually in current practice, the initiating conditions of energy transfer from the hammer to the pile are simply assumed and the vibration attenuation is taken as a function of the distance from the source, omitting the gradual penetration of the pile into soil layers with variable dynamic resistances, an aspect that governs both the propagation of waves in the pile (A) and the dynamic pile-soil interaction (A to B) in Fig. 1. This is an unnecessary and unacceptable oversimplification of the actual condition, because, as will be shown, the initiating conditions of force transfer can be rationally developed and included in an analysis.

The dynamic soil-structure interaction of piled foundations at small strains, such as the dynamic response of machine foundations, is described extensively in the literature (e.g., Novak and Janes 1989). However, for dynamic pile-soil interaction at large strain levels (as will be the case during pile penetration), only limited information is available. Yet, this is the case applicable to vibrations induced during pile driving (Massarsch 2005).

Stress-wave Measurements During Pile Driving

Major advances have been made in measuring and analyzing dynamic wave propagation in piles during impact driving (Goble et al. 1968, 1980; Goble 1995). Dynamics measurements consist of attaching pairs of strain gages and accelerometers to the pile below the pile head. The strain measurement corresponds to the stress (force) in the pile, and the acceleration measurement, integrated, provides the particle

velocity during the impact. The event is brief, but its duration is measurable and is illustrated in curves of force versus time, so-called wave traces. As indicated by many (e.g., Fellenius 2006), a key to the understanding and analysis of the measurements is that the ratio between the force and the acceleration integrated to velocity is proportional to the pile impedance, Z^P, as expressed in Eq. 2.

$$Z^P = \frac{E^P A^P}{c^P} = A^P c^P \rho^P \qquad (2)$$

where Z^P = impedance of pile
E^P = modulus of elasticity of pile material
A^P = pile cross section area
c^P = velocity of stress wave in pile
ρ^P = density of pile material

Note that in the following, to avoid confusion between different notations, symbols referring to pile (P) and hammer (H) will be indicated by raised indices while notations referring to soil properties will be denoted by lowered indices.

In the absence of any resistance along the pile, the force trace is exactly the same as the velocity trace multiplied by pile impedance—the two traces overlap. However, during pile penetration, soil resistance is not absent. When the impact wave propagating down the pile encounters resistance, a reflected stress wave is generated that propagates upward from the resistance location. The interesting part is that, when the reflected wave reaches the gage location, in superimposing the strain from the hammer energy still entering the pile, strain increases — the force curve rises. At the same time, the reflected wave slows down the pile and the velocity reduces — the curve for velocity times impedance trace dips. The effect is a separation of the two curves, which is a measure of the total (dynamic and static) soil resistance at the location of the reflection along the pile.

The resistance to the driving can be considered in terms of penetration (blow count) or driving resistance (force). (Note that it is only the dynamic resistance which gives rise to ground vibrations—emitted from the pile shaft and/or pile toe to the surrounding soil layers). When plotting the measurement against time scaled to the length of time for the impact wave to reach the pile toe, i.e., in *L/c* units, a visual display is obtained of the magnitude and location along the pile of the encountered soil resistance — static plus dynamic combined. To illustrate, Figs. 2 and 3 present dynamic records from the driving of two piles, one meeting mostly shaft resistance, and one mostly toe resistance. Fig. 2A shows measured force and velocity wave traces and calculated transferred energy trace. Fig. 2B shows calculated Wave Down trace, the mean of the two wave traces and the force entering the pile from the hammer, and calculated Wave Up trace, half the difference between the wave traces, i.e. the mobilized static and dynamic resistance. Fig. 3A shows the measured force and velocity wave traces. Fig. 3B shows calculated Wave Down traces.

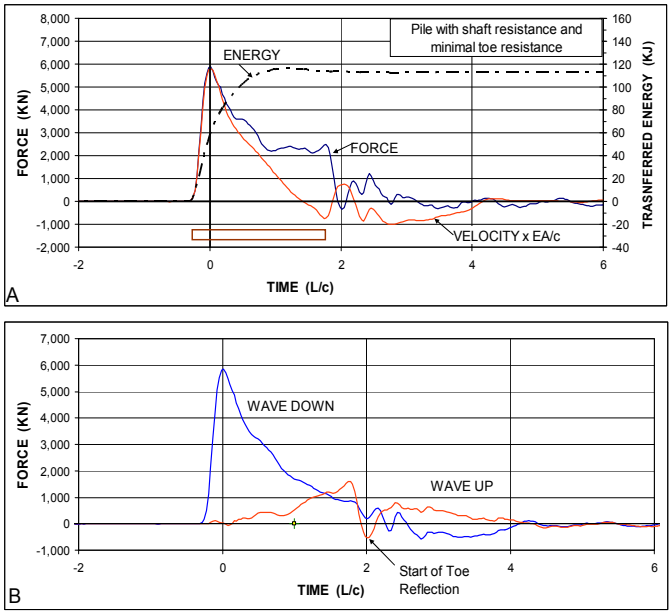

Fig. 2. Examples of force and velocity wave traces measured in a 30 m long pipe pile driven into silty sand in British Columbia and encountering mostly shaft resistance. (Data courtesy of AATech Scientific Inc.).

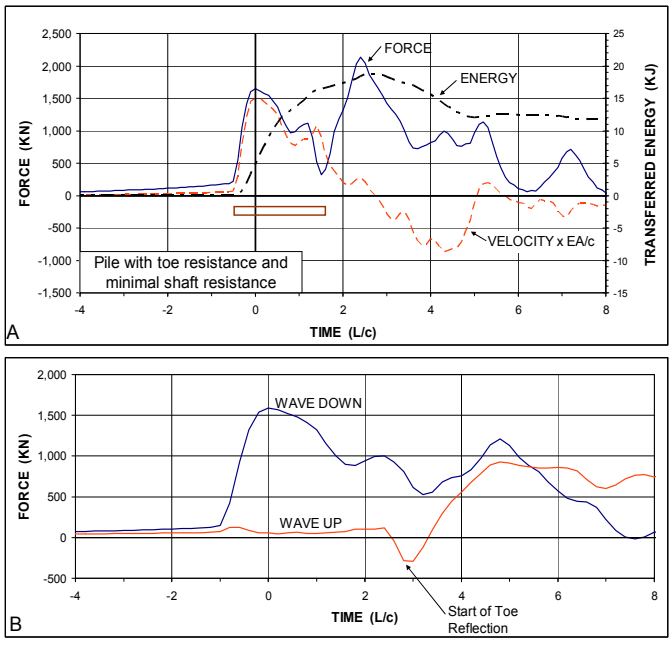

Fig. 3. Examples of force and velocity wave traces measured in an 8 m long H-pile driven through soft soil into weathered bedrock in Oklahoma and encountering mostly toe resistance. (Data courtesy of AATech Scientific Inc.).

By analyzing the records with the CAPWAP program (Rausche et al., 1985), the total shaft and toe resistances can be numerically determined and the static resistance separated from the dynamic. Usually, dynamic monitoring during the driving of a pile is continuous until the end of driving. Information on the conditions for when the pile toe enters a specific layer can then be subjected to a CAPWAP analysis and provide the reference to a vibration analysis.

Note, that a routine CAPWAP analysis aims to determine the distribution of static resistance, while a vibration analysis requires the distribution of dynamic resistance, which is normally not reported in a CAPWAP analysis. However, also the dynamic resistance can easily be established from the CAPWAP results. Thus, stress-wave measurements in combination with ground vibration measurements, could provide valuable quantitative information regarding the transmission of vibrations during pile penetration.

Empirical Vibration Attenuation Concepts

Theories regarding ground vibration attenuation were initially developed for rock blasting applications. Field measurements of ground surface vibrations indicated that these could be related to the energy released in a blast (Wiss 1981). Empirical relations were developed, showing magnitude of blasting vibration as function of energy release. Similar relations were developed for the prediction of vibrations caused by other types of energy sources, for example, pile driving or soil compaction, which are still widely used (Jedele 2005). Attewell and Farmer (1973) analyzed results of measurements in a variety of soils of vibration induced by the driving of different types of piles. They suggested that a conservative energy-based estimate of vibration velocity, v, at distance, r, from the energy source (pile) can be made from the relation expressed by Eq. 3.

$$v = k\frac{\sqrt{W}}{r} \tag{3}$$

where v = vibration velocity (m/s)
W = energy input at source (J)
k = an empirical vibration factor ($m^2/s\sqrt{J}$)
r = distance from pile (m)

The vibration velocity is not defined in terms of direction of measurement (vertical, horizontal, or resultant of components). Rather surprising, they reached the conclusion that the attenuation of ground vibration amplitude with distance from a pile is largely independent of the type and strength or stiffness of the ground. An additional important aspect, which is not considered in Eq. 3, is whether the nominal hammer energy or an adjusted energy value should be used. Note also that the empirical factor, k, has caused some confusion in the literature as it is not dimensionless. In many cases, the units applied to the vibration factor were not in agreement with those of the vibration velocity. Attewell and Farmer (1973) did not indicate which distance to be used in Eq. 3. Therefore, often the shortest distance from the pile on the ground surface to the point of observation is selected by practicing engineers, disregarding the depth of pile penetration (thus not considering the actual location of the source of the vibrations).

Brenner and Viranuvut (1975) used Eq. 3 to compare results of vibration measurements from pile driving in terms of vibration velocity with information from projects reported in the literature, as shown in Fig. 4. The results indicate values of the empirical factor, k, ranging from 0.3 through 4.0 (velocity in mm/s).

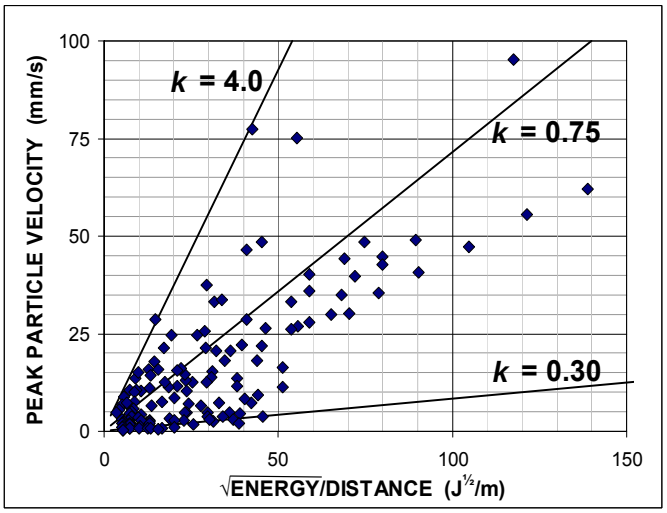

Fig. 4. Attenuation of peak particle velocity versus scaled energy (data from Brenner and Viranuvut 1975).

As shown in Fig. 4, the scatter of values is large and would be unacceptable for most conventional geotechnical design applications. Yet, the energy-based relation of Eq. 3 is still frequently used for prediction of ground vibrations (Woods and Jedele 1985; Jedele 2005).

One of the most widely referenced publications on this subject is a state-of-the-art paper by Wiss (1981) on construction vibrations, who proposed Eq. 4, a relation similar to Eq. 3, where the peak particle velocity, v, is expressed as a function of the distance from the energy source, r (when the exponent, n, equals unity, "k" and "K" in Eqs. 3 and 4 are identical). Wiss (1981) used imperial units in Eq. 4, which adds to the confusion when applying the equation in practice.

$$v = K\left(\frac{D}{\sqrt{E}}\right)^{-n} \tag{4}$$

where v = peak particle velocity (inches per second)
K = intercept value of vibration amplitude (inches/s) at "scaled distance" $D/\sqrt{E} = 1$ (ft/lb)$^{1/2}$
n = slope or attenuation rate
D = distance from source (feet)
E = energy input at source (in foot-pounds) or explosive charge weight per delay (pounds)

The value of the attenuation rate, n, in Eq. 4 generally lies between 1.0 and 2.0 with a commonly assumed value of 1.5 — units unknown. Note that the expression (Eq. 4) is ambiguous as the value of the exponent, n, affects K. This makes the comparison of the K-values impossible for different attenuation rates. Same as Attewell and Farmer (1973), Wiss (1981) provides neither guidance on how the distance should be chosen when a pile penetrates into the ground, nor a definition of the driving energy. This aspect will be discussed in the following.

Influence of Pile Penetration Depth

The above presented energy-based relationships refer to the attenuation of vibrations from the vibration source to the observation point. However, in the case of pile driving, the location of the source of the vibration energy is not well defined (in contrast, for example, to the case for blasting) as vibrations can be emitted from the shaft or the toe of the pile — or from both at the same time — and also more from some layers penetrated by the pile and less from others. Thus, as the pile encounters dense soil layers close to the ground surface at the beginning of driving and then continues into weaker soil, the depth of the energy source will change and, accordingly, so will the distance from the source to the observation point. However, most cases reporting results from vibration measurements use the horizontal distance at the ground surface in correlating energy source and vibrations. The problem is illustrated in Fig. 5, showing two ground surface measuring points, A and B, located at different distances from a long pile.

Point A is located close to the pile, while the distance to Point B at the end of driving may correspond to more than one pile length. When the horizontal distance is used for the vibration measurements at Point A during the penetration of the pile, neglecting the gradually increasing pile penetration length, the vibration amplitude will be overestimated due to a much shorter assumed propagation distance. The effect of the neglect is smaller for a measuring point away from the pile location, such as at Point B. In most cases, problems associated with vibrations from pile driving occur at distances up to approximately one to two pile lengths, which cases are representative for a point located between A and B. It is obvious that consistent results cannot be expected from analyses based on horizontal distance values.

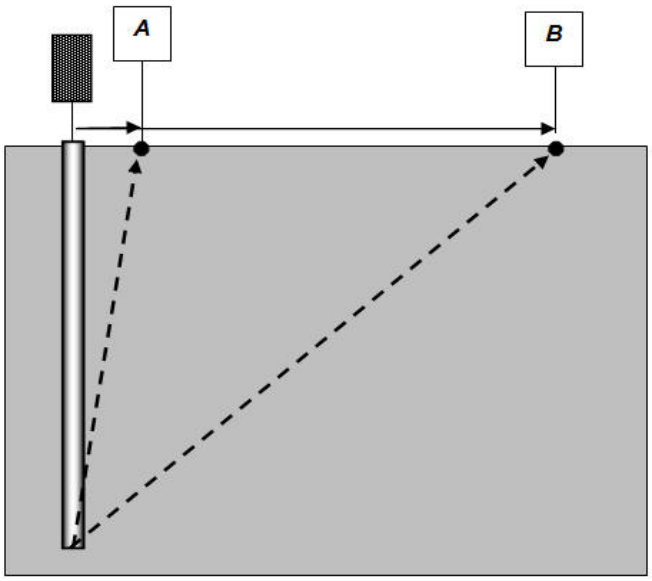

Fig. 5. Influence of pile penetration depth on the distance to measuring points at two locations, A and B.

The distance to the vibration source depends also on the variation of soil resistance along the pile shaft, R_S and at the pile toe, R_T. This case is illustrated in Fig. 6, showing two penetration resistance curves, Cases 1 and 2, which typically would be obtained from pile driving records or, for predictions, be determined from in-situ tests, such as the cone penetrometer, or be calculated in a wave equation analysis.

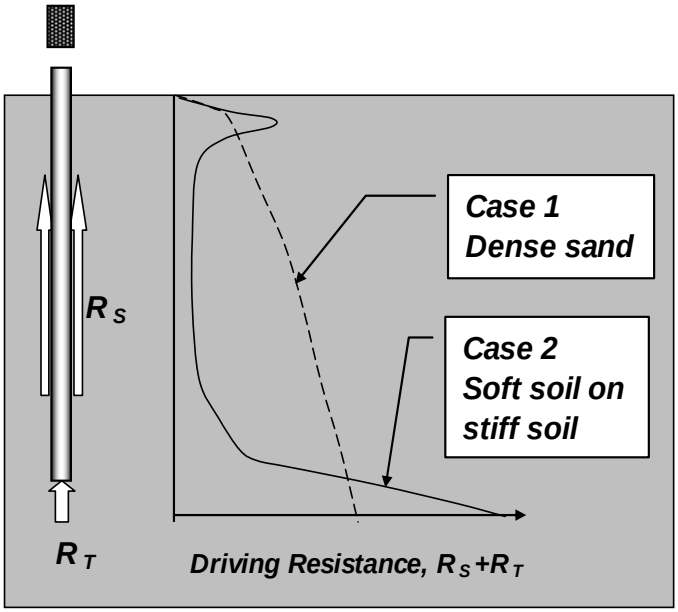

Fig. 6. Conceptual picture of soil resistance along the shaft, R_T and toe, R_S when driving a pile into dense sand and soft clay on a stiff layer, respectively. Note, the driving resistance is indicated in units of force, not in units of penetration resistance ("blow count").

In Case 1, it is assumed that the pile is driven into a sand deposit with gradually increasing density, where a significant amount of the resistance will be generated along the shaft of the pile, especially if a group of piles is driven, resulting in gradual soil densification. Waves will then propagate mainly as cylindrical shear waves, with wave attenuation similar to surface waves (New 1986, Selby 1991, Massarsch 1992).

In Case 2, it is assumed that the pile is driven into a clay layer with a dry crust (or surface fill). As the pile driving begins, the vibrations will travel along the ground surface in the form of surface waves. When the pile toe has penetrated into the soft clay layer, ground vibrations will decrease and the vibrations may even become negligible at this time, as little energy can be transferred through the surrounding remolded soil. During the final phase (termination) of pile driving (hard driving is assumed), when the toe of the pile has reached the dense bottom layer, most of the soil resistance will be generated at the pile toe, and the vibrations will mainly be transmitted in the form of spherical waves from the pile toe.

Simple stress-wave measurements, as discussed above, can provide valuable insight into the magnitude and distribution of dynamic soil resistance and vibration transmission along the pile shaft and the pile toe, respectively. Obviously, during impact driving, vibrations can be transmitted along the pile shaft and/or at the pile toe, depending on the soil conditions. The location of the source of vibration emission (origin of dynamic soil resistance) will change during pile penetration. Information on the geotechnical conditions, such as soil stratification and strength/stiffness properties, are therefore essential when analyzing ground vibrations and need to be incorporated in a realistic prediction model. Moreover, pile driving can generate vibrations simultaneously in the form of cylindrical waves and surface waves from the pile shaft and spherical waves from the pile toe. This aspect is important and therefore discussed in detail below.

DYNAMIC PILE-SOIL INTERACTION

Velocity-dependent Soil Resistance

A key aspect of understanding the source of ground vibrations, which is not generally appreciated by geotechnical engineers, is the fact that the intensity of vibrations in the ground depends on the velocity-dependent (dynamic) soil resistance generated along the shaft and at the pile toe. The dynamic soil resistance defines the maximum value of vibration velocity which actually can be transmitted at the pile-soil interface. A simple example can illustrate the concept. When a pile is pushed at very slow penetration speed into the ground (e.g., static loading test), the total soil resistance is composed of the static shaft and toe resistances, respectively. Of course, as no dynamic forces are involved, no ground vibrations will be transmitted to the surrounding soil layers. When the pile is driven into the ground by impact, "dynamic" velocity-dependent soil resistance will develop that will increase the total driving resistance and at the same time give rise to ground vibrations.

The analysis of energy propagation from the pile into the surrounding soil is based on elasticity theory. However, this concept is strictly only applicable when soil deformation (strain) is very low, which is the case for properly designed and functioning machine foundations. During pile driving, the soil along the shaft and at the toe is in a state of failure, as it is subjected to large strains (plastic deformations occur). The aspect of strain softening of soils near the pile could be readily incorporated in a more elaborate prediction model. In addition, especially along the shaft, the soil will be remolded. Therefore, only part of the energy applied to the pile head and transmitted to the pile will cause vibrations in the surrounding soil, a fact which is not recognized in the empirical, energy-based prediction model. As will be described in this chapter, it is possible to estimate the vibrations which can be transmitted from the pile shaft and the pile toe using rationally developed correction factors.

The dynamic soil resistance can be a major component of the total driving resistance, and its variation during pile penetration can be determined accurately by stress-wave measurements. As yet, however, in assessing ground vibrations, the profession has not considered this aspect and has not taken advantage of the important information.

Two main factors must be considered when determining ground vibrations: the dynamic force in the pile generated by the impact and the dynamic soil resistance at the pile-soil interface, which is a function of the pile physical velocity (relative velocity between the pile and the soil) and the dynamic soil properties. The maximum value of the dynamic force propagating down the pile can be reliably measured or estimated with sufficient accuracy. The maximum value of the dynamic soil resistance can be established from the dynamic properties of the soil (soil impedance and soil damping). The ratio between the impact force in the pile and the dynamic soil resistance is the fundamental parameter which controls ground vibrations, and it can be estimated and used to assess the transmission of ground vibrations from the pile to the surrounding soil layers.

For understanding ground vibrations induced by impact pile driving, it is imperative to apply the fundamentals of pile dynamics and dynamic pile-soil interaction. These will therefore be outlined in the following.

Pile Hammer Efficiency and Energy Ratio

Hammer efficiency is defined as the ratio between the kinetic energy of a gravity hammer (ram) on impacting the helmet cushion (or, for a diesel hammer on impacting the anvil) over the kinetic energy of the ram free-falling the same distance without loss of energy. Hammer efficiency can only be determined by field measurements of impact velocity (Rausche, 2000). The hammer efficiency should not be used to imply that one hammer is better or worse than another. However, it is an important input to a wave equation analysis of pile driving. In the absence of any measurements, the practice applies an approximate hammer efficiency input, a factor, F^H, chosen based on experience. Table 7 presents an array of recommended ranges of efficiency factors according to Rausche (2000). It should be noted that, for a conservative prediction, it is recommended to use the larger value of the ranges, unless otherwise prompted.

Table 7. Recommended values of hammer efficiency factor, F^H (after Rausche, 2000)

Hammer Type	Hammer Efficiency Factor, F^H
Free-fall hammer (free release)	0.90 – 0.95
Single-acting air/steam hammer:	
Steel piles (end of driving)	0.55 – 0.70
Concrete or wood piles (end of driving)	0.40 – 0.60
Double and differential acting air/steam hammers:	
Steel piles (end of driving)	0.35 – 0.50
Concrete or wood piles (end of driving)	0.30 – 0.45
Diesel hammers	
Steel piles (end of driving)	0.30 – 0.40
Concrete or wood piles (end of driving)	0.25 – 0.30
Hydraulic drop hammers (self-monitored)	0.85 – 0.95
Hydraulic drop hammers (other types)	0.55 – 0.85

Energy ratio, or transferred-energy ratio, is the ratio between the maximum energy transferred through the driving system (air, anvil, hammer cushion, pile cushion, etc.) to the pile over the potential or positional energy of the impact. The transferred energy is obtained from dynamic measurements as the integration of measured force times velocity times pile impedance.

Force Imparted to Pile

A dynamic model of pile driving forces is shown in Fig. 7, which can be analyzed using stress-wave theory (e.g., Smith 1960; Goble et al. 1980; Broms and Bredenberg 1982; Massarsch 2005). The model shows a pile being driven with an impact hammer having a mass, M^H, and a height-of-fall, h. The impact mobilizes soil resistance along the pile shaft, R_S, and at the pile toe, R_T. The relationship between the axial force, F_i, and the particle velocity (i.e., physical velocity) of the pile, v^P, as defined by Eq. 5, is a starting point for the analysis. Note that the model is a simplification of reality, showing velocities as rectangular waves, as opposed to increasing to a peak and attenuating thereafter.

$$F_i = Z^P v^P \tag{5}$$

where F_i = force in pile
v^P = particle velocity (physical velocity) of pile

Note, that several notations are shared between equations. In order to save space, notations are defined only at their first mention below the equation. All notations are provided in the Notation Appendix.

The pile impedance, Z^P, can be determined from Eq. 6. See also Eq. 2.

$$Z^P = A^P c^P \rho^P \tag{6}$$

where c^P = velocity of stress wave in pile
ρ^P = density of pile material
A^P = cross section area of the pile

Equations 2 and 6 can be used to calculate the axial impact force in a pile based on measurement of the particle velocity during driving. The parameters defining the propagation of a stress wave caused by the impact of a drop hammer on a pile are given in Fig. 7.

At impact, the particle velocity, v_0, of the hammer (the ram) with mass, M^H, hammer length, L^H, and a height-of-fall, h, while the particle velocity of the pile head is zero. The velocity of the hammer immediately before (i.e. at) impact, v_0, can be estimated from the hammer height-of-fall, assuming no loss of energy in the fall, as expressed in Eq. 7.

$$v_0 = \sqrt{2gh} \tag{7}$$

where v_0 = velocity of hammer at impact
g = acceleration of earth gravity.
h = hammer-height-of-fall

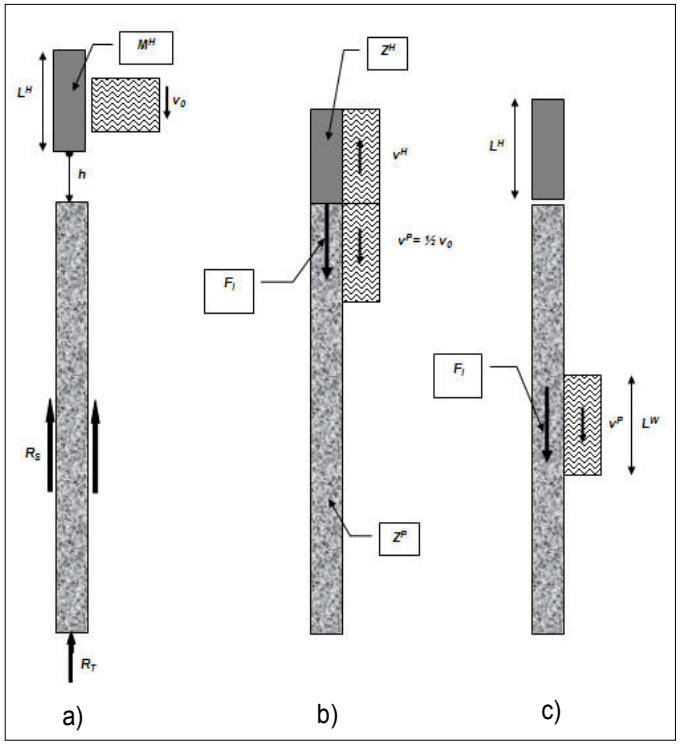

Fig. 7. Definition of parameters governing stress wave propagation in piles.

When the hammer strikes the pile, a stress wave will be generated simultaneously in the pile and in the hammer, as indicated in Fig. 7b. The hammer velocity starts to slow down, by a velocity denoted v^H, while the pile head starts to accelerate, gaining a velocity of v^P. Since the force between the hammer and the pile must be equal, applying Eq. 5 yields the relationship expressed in Eq. 8.

$$Z^H v^H = Z^P v^P \tag{8}$$

where Z^H = impedance of hammer (ram)
v^H = particle velocity of wave reflected backup the hammer

At the contact surface, the hammer velocity—decreasing—and the pile head velocity—increasing—are equal, as expressed in Eq. (9).

$$v_0 - v^H = v^P \tag{9}$$

Note, the change of hammer particle velocity is directed upward, while the velocity direction of the pile head is downward. The hammer and the pile will remain in contact only for a short time, the impact time. Combining Eqs. 8 and 9 and rearranging the terms, yields Eq. 10.

$$v^P = \frac{v_0}{1 + \frac{Z^P}{Z^H}} \tag{10}$$

Inserting $Z^H = Z^P$, into Eq. 10 yields Eq. 11, which shows that when the impedances of the hammer and the pile are equal, the peak particle velocity of the pile, v_P, will be half the hammer impact velocity, v_0, (the velocity immediately before touching the pile head).

$$v^P = 0.5 v_0 \tag{11}$$

The particle velocity in the pile (and, therefore, the force in the pile) is not affected by the hammer mass, M^H, but rather by the hammer height-of-fall, h (Eq. 7), and the impedance ratio of the impact hammer and the pile. However, neither the height-of-fall nor the impedance ratio is normally mentioned when measurements of ground vibrations are reported in the literature. Combining Eqs. 5 and 11 yields Eq. 12 which expresses the magnitude of the impact force, F_i, the peak force, at the pile head for equal impedance of hammer and pile. Note, in the terminology common in dynamic pile testing, the time of impact is the instant of the peak force (occurs when acceleration becomes negative).

$$F_i = Z^P 0.5\, v_0 \tag{12}$$

Another important aspect of pile driving is the duration of the impact, as this determines the length of the propagating stress wave. The upward traveling stress wave in the hammer caused by the impact with the pile is reflected when the front reaches the top of the hammer. The upper end of the hammer is a free end, which means that the force is equal to zero at all times. Therefore, the upward traveling wave reflected from the pile head is now reflected as a tension wave. The time, t, during which the pile head and the hammer are in contact is the time it takes for the strain wave to travel the length of the hammer, L^H, twice, i.e., from the top of the hammer to the bottom end and back up to the top, is expressed in Eq. 13.

$$t = \frac{2L^H}{c^H} \tag{13}$$

where t = duration of impact (i.e., duration of contact between hammer and pile head)
L^H = length of hammer
c^H = velocity of stress wave in hammer

Then, if the impedances of the hammer and the pile are equal, during the same time interval, the stress wave will travel the length expressed in Eq. 14, which defines the length of the stress wave in the pile (and the length of pile along which vibrations are transferred to the surrounding soil).

$$L^W = t\, c^P \tag{14}$$

where L^W is the length of the stress wave propagating down the pile. If the materials in the hammer and the pile are different, but the impedances are the same due to difference in cross-section and material, the length of the stress wave in the pile will be as expressed in Eq. 15.

$$L^W = 2L^H \frac{c^P}{c^H} \tag{15}$$

Equation 15 is of practical importance for calculation of ground vibrations, because the length of the impact time and length of the wave propagating down the pile determine the length of time during which the force is transmitted to the pile shaft and out into the soil. In conclusion, it can be stated that the impact velocity (which depends on the hammer height-of-fall) and the length of the pile hammer (which governs the duration of the impact) are the two most important pile driving parameters governing ground vibrations.

DYNAMIC SOIL RESISTANCE AT SHAFT AND TOE

During pile penetration, dynamic soil resistance will be generated along the pile shaft and at the same time at the pile toe. This important aspect, which governs ground vibration emission during pile driving, is now discussed and equations are given showing how to estimate dynamic resistance values.

Dynamic Soil Resistance along Pile Shaft

The dynamic soil resistance along the pile shaft, R_S, can be estimated if the specific soil impedance (shear wave), z_S, along the pile shaft and the contact area, between the shaft and soil, S, are known, as indicated in Eq. 16.

$$R_s = z_S\, v^P\, S^P \tag{16}$$

where R_S = dynamic soil resistance along the pile shaft
z_S = specific soil impedance for shear waves
v^P = particle velocity of the pile
S^P = contact area between the shaft and soil

The specific soil impedance, z_S, is determined from Eq. 17.

$$z_S = c_S\, \rho_{soil} \tag{17}$$

where c_S = shear-wave velocity of the soil at the pile-soil interface
ρ_{soil} = total (bulk) soil density

The specific soil impedance, z_S, is a material property with the units kNs/m^3 (note, "z" written in lower case letter) and should not be confused with for instance the pile impedance Z^P, which also depends on the cross section area of the pile with the units kNs/m.

Due to the relative movement between the pile and the soil, a zone surrounding the pile shaft will be disturbed and often remolded. Consequently, even at relatively small strains, the soil stiffness (and thus the wave velocity) decreases. The effect of shear strain on the shear wave velocity depends on soil type, expressed by the Plasticity Index, PI, and driving resistance, as indicated in Fig. 8. As discussed by Massarsch (2004, 2005), when selecting a representative value for the shear wave velocity, a reduction of the small-strain shear-wave velocity, R_C, needs to be introduced. It is also necessary to apply a factor R_R, which is representative for the disturbance and remolding effects.

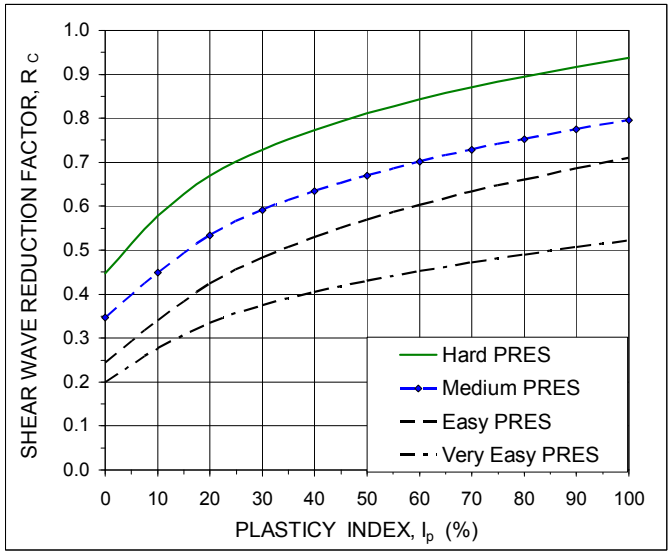

Fig. 8. Shear wave velocity reduction factor, R_C as function of plasticity index, I_P, for different conditions of penetrations resistance, PRES, modified from Massarsch (2005).

The dynamic shaft resistance, which is the source of cylindrical (shear) waves emitted from the pile shaft, can now be determined by combining Eqs. 12, 16, and 17 and assuming that the pile length in contact with the soil is equal to the length of the stress wave in the pile. Then, for a pile with a cylindrical shape and a diameter, b^P, the dynamic shaft resistance, R_S, is expressed in Eq. 18.

$$R_S = 0.5 v_0\, R_c\, R_R\, c_S \rho_{soil}\, b^P \pi\, L^W \tag{18}$$

where R_C = reduction factor for strain-softening
v^P = particle velocity of the ram at impact
R_R = reduction factor for remolding/disturbance
b^P = pile diameter

Typical values of the P-wave (stress wave) and S-wave (shear wave) velocities at small strains ($<10^{-3}$ %) are given in Table 8. Note that the wave velocity in soil layers depends on several factors, such as the effective stress, void ratio, preconsolidation stress, etc., and normally increases with depth. Therefore, the values in Table 8 are approximate and should be used only for preliminary assessment but can be determined by empirical methods or field measurements.

Normally, the shear wave velocity is not affected by the presence of water in the ground. However, in the case of pile driving, the shear wave velocity can decrease due to excess pore water pressure and soil disturbance. In contrast, the P-wave (compression) velocity of soils below the groundwater table corresponds to that of water (assumed to 1,450 m/s). During penetration of the pile, the shaft resistance diminishes as a result of soil disturbance (remolding). Due to this and because of the large strains imposed, it would be wrong to apply the low-strain condition ("elastic") shear wave velocity as listed in Table 8 to Eq. 18, because this would yield too high dynamic resistance values (in contrast to the design of, for example, machine foundations which operate in the elastic range and where small-strain values apply).

Table 8. Range of compression (P-) and shear (S-) wave velocities at small strains for different soil types

Soil Type	P-Wave Velocity (m/s)	S-Wave Velocity (m/s)
Water	1,450	0
Glacial till	600 - 1,800	300 - 600
Dry gravel	500 - 1,000	250 - 400
Saturated gravel	1,450	300 - 400
Dry sand	300 - 600	150 - 200
Saturated sand	1,450	150 - 250
Silts and stiff clays	1,450	100 - 200
Plastic clay	1,450	50 - 100
Organic soils	1,450	30 - 50

The resistance along the pile during penetration will also be affected by stress changes in the soil during driving. This is most significant in sensitive, fine-grained soils, where large excess pore water pressure can develop. If pile driving is interrupted, for example in connection with splicing of piles, the excess pore water pressure can dissipate rapidly and increase the shaft resistance. This effect can result in increased ground vibrations when the driving is resumed. Also in dense granular soils, the soil strength and stiffness along the pile shaft will most likely be reduced when the pile-soil interface is sheared. On the other hand, if a group of piles is driven into loose or medium dense sand, gradual densification and increased lateral earth pressure may cause a significant increase of shaft resistance. Note that stress-wave measurements would provide directly applicable, quantitative information regarding the resistance distribution during pile penetration.

Vibration Transmission Along Pile Shaft

It is important to express in quantitative terms how much of the potential driving energy can actually be transferred to the surrounding soil. There are two limiting situations. The maximum force applied to the pile head can be estimated from Eq. 5. On the other hand, the dynamic soil resistance, R_S, which depends on the soil impedance adjacent to the pile shaft, is the upper limit of vibrations which can be transferred to the surrounding soil. It is useful to define a ratio of the dynamic soil resistance along the pile shaft, R_S, divided with the impacting force, F_i (Eq. 5), called shaft vibration transmission efficacy, E_S. If, again, it is assumed that the pile has cylindrical shape with diameter, b, and effective contact length, L^W, then, division of Eq. 18 by Eq. 5 combined with Eq. 2 yields Eq. 19.

$$E_S = 2\, R_c\, R_R\, \frac{c_S}{c^P}\, \frac{\rho_{soil}}{\rho^P}\, \frac{L^W}{b^P} = 2 R_c\, R_R\, \frac{z_S}{z^P}\, \frac{L^W}{b^P} \qquad (19)$$

where E_S = vibration transmission efficacy along the pile shaft = R_S/F_i
z_S = specific soil impedance for shear waves
z^P = specific impedance of pile

Note that the term "impedance" is almost unknown to most geotechnical engineers in spite of its great practical importance! Equation 19 shows that the length of the stress wave (which is the effective contact length of the stress wave with the soil, a function of hammer length) governs the transmission efficacy of vibrations from the pile shaft to the surrounding soil. That is, the transmission efficacy is a function of the ratio of soil to pile impedance. A typical upper range of reduction factor for disturbance (which will provide conservative estimates of ground vibrations) is in the range 0.2 to 0.4, as indicated in Fig. 9.

It should be noted that E_S cannot be larger than unity, i.e., the dynamic soil resistance controls the maximum force that can be transmitted to the soil. For an example of the range of typical values for E_S in different soils and driving conditions, assume that the average density of a soil, ρ_s, is 1,800 kg/m^3, and that the density of the pile material, ρ^P, is 2,450 kg/m^3 (a concrete pile is assumed). The relationship between E_S and the contact length of the pile shaft with the surrounding soil, L^W/b, for this pile is shown in Fig. 9. Two values of the shear

wave velocity reduction factor, R_C have been chosen (0.2 and 0.4). The E_s-values in Fig. 9 are considered to be upper limits, as the reduction effect of soil disturbance and remolding is not included.

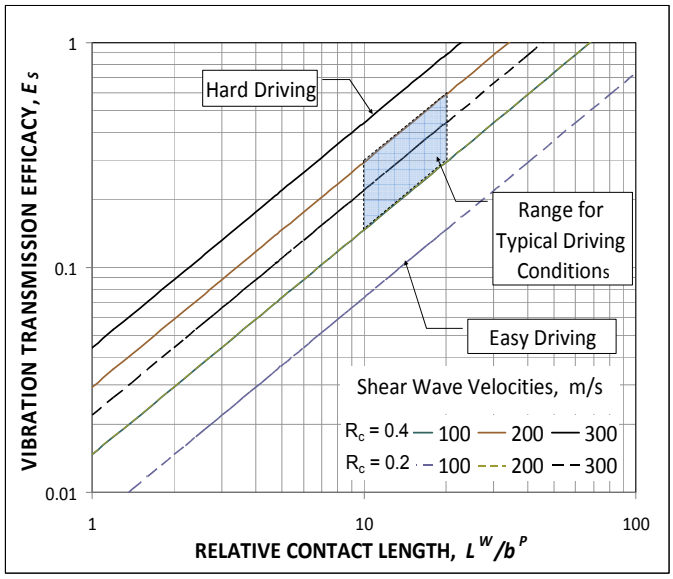

Fig. 9. Vibration transmission efficacy, *E_S, along the shaft of a concrete pile as function of relative pile contact length for different driving conditions, assuming a cylindrical pile driven into soils with different shear wave velocity (Table 8).*

The vibration transmission efficacy can be determined from Eq. 19 for any pile shape and effective contact length of the pile shaft. It is evident that the impedance ratio z_s/z^P and the L^W/b-ratio are important factors which need to be considered when determining the emission of cylindrical waves from the pile shaft. For example, the L^W/b^P-ratio will be large in the case of sheet piles or H-piles, as these have a larger average diameter (read: surface area) than cylindrical piles. It must be expected, therefore, that ground vibrations will be higher when driving sheet piles as opposed to driving cylindrical piles.

During pile penetration, friction between the pile shaft and granular soil can also give rise to a horizontal vibration component, which is important in the case of vibratory driving, but is usually neglected in the case of impact driving.

Dynamic Soil Resistance at Pile Toe

The dynamic force at the pile toe, R_T, which is the source of spherical waves emitted from the pile toe, can be estimated from Eq. 20 (Goble et al. 1980).

$$R_T = J_c \, Z^P \, v^P \tag{20}$$

where R_T = dynamic portion of the driving resistance at the pile toe
J_c = dimensionless damping factor
Z^P = pile impedance (Eq. 2)
v^P = particle velocity in the pile

The damping factor, J_c, is generally considered to depend only on the dynamic properties of the soil and independent of the pile type. However, Fellenius et al. (1989) showed that J_c-factors correlated to pile capacity were different for different piles (different impedance) tested at the same site.

Iwanowski and Bodare (1988) derived J_c analytically, using the model of a vibrating circular plate in an infinite elastic body to describe the interaction between the pile toe and the surrounding soil. They made the important observation that J_c depends not only soil alone but also on the ratio between the pile impedance, Z^P, at the pile toe and the soil impedance for P-waves, Z_P, as shown in Eq. 21.

$$J_c = 2\frac{Z_P}{Z^P} \tag{21}$$

The soil impedance, Z_P, is defined in Eq. 22, which is similar to Eq. 6.

$$Z_P = A^P \, c_P \, \rho_{soil} \tag{22}$$

where Z_P = soil impedance for P-waves at the pile toe
A^P = cross section area of the pile toe
c_P = velocity of P-wave in the soil

[Note, the two impedance symbols, Z^P and Z_P, the pile impedance and the soil impedance, respectively, can easily be confused with each other].

The soil impedance for P-waves, Z_P, depends on the cross-section area of the contact between the pile toe and the underlying soil and is not the same as the specific soil impedance, z_P, for P-waves, which is a material property of the soil and does not involve the pile geometry. Also, the soil impedance is strain-dependent and needs to be adjusted for strain level during pile driving/testing. The dynamic portion of the driving resistance at the pile toe, R_T, can now be readily calculated by combining Eqs. 20 and 21 to arrive at Eq. 23.

$$R_T = 2 \, Z_P \, v^P \tag{23}$$

The damping factor J_c does not appear in Eq. 23, in contrast to the widely used relationship given in Eq. 20. Indeed, the soil impedance, Z_P, of the P-wave is sufficient to determine the dynamic resistance at the pile-soil interface. Note that the P-wave depends on the degree of water saturation (ground water conditions) in loose soils, an aspect which is not generally appreciated.

By combining Eqs. 11 and 23, and assuming that the hammer and pile impedances are equal, the dynamic toe resistance, can now be expressed in terms of the hammer impact velocity, v_0, as shown in Eq. 24.

$$R_T = Z_P \, v_0 \tag{24}$$

Vibration Transmission at Pile Toe

The ratio of the dynamic soil resistance at the pile toe, R_T, divided with the impacting force, F_i (Eq. 5), is called toe vibration transmission efficacy, E_T. Division of Eq. 24 by Eq. 12 yields Eq. 25a

$$E_T = 2\frac{Z_P}{Z^P} \tag{25a}$$

where E_T = vibration transmission efficacy at the pile toe = R_T/F_i

If it is assumed that the pile shaft and the pile toe have the same cross section area, Eq. (25a) can be simplified to

$$E_T = 2\frac{c_P}{c^P}\frac{\rho_{soil}}{\rho^P} = 2\frac{z_P}{z^P} \tag{25b}$$

where z_P = specific soil impedance for P-waves
z^P = specific impedance of pile material

Note that the specific pile impedance, z^P is a material property, as pointed out above, and should not be confused with the pile impedance, Z^P. In the case of driving a pipe pile, the contact area with the soil at the pile toe can be different to the cross section area of the pile and in that case, Eq. 25a should be used. During pile penetration, the soil stiffness (and therefore the soil impedance at the pile toe) will change. This effect is taken into account by introducing an empirical factor, R_R, which, inserted into Eq. 25a yields Eq. 25c.

$$E_T = 2R_R\frac{c_P}{c^P}\frac{\rho_{soil}}{\rho^P} = 2R_R\frac{z_P}{z^P} \tag{25c}$$

where R_R = an empirical factor that takes into account soil compaction (loose, coarse-grained soils) or disturbance (clays) at the pile toe

At present, limited information is available regarding the exact value in different soils of the factor, R_R. However, it can be assumed that in loose and medium dense coarse-grained soils due to compaction or densification, R_R will increase with increasing driving resistance. As a preliminary indication, a conservative value of $R_R = 2$ should be assumed in such soils. In overconsolidated clays, pile driving will gradually reduce the soil stiffness (impedance) at the pile toe and it is safe to assume R_R = 0.2 – 0.5. For conservative predictions, it is recommended to use upper boundary values. However, it is suggested to determine this parameter based on field tests.

Equation 25 shows that the vibration transmission efficacy increases with decreasing pile impedance and increases with increasing soil density. For example, driving a concrete pile with an assumed wave velocity of 4,000 m/s and a bulk density of 2,400 kg/m^3, into a saturated soil with a P-wave velocity of 1,450 m/s and a bulk density of 1,800 kg/m^3, then, the toe vibration transmission factor, E_T, becomes 0.25. If instead, the pile is driven into a glacial till with a P-wave velocity of 1,500 m/s and a density of 2,200 kg/m^3, the toe factor becomes 0.35. If the pile is a steel H-pile with a wave velocity of 5,000 m/s and a density of 7,800 kg/m^3, then, the toe factor becomes 0.06 and 0.07, respectively. Obviously, the pile material and impedance are decisive aspects of the vibration transmission.

Comparison with Field Data

The damping factor, J_c which is widely used in pile dynamics, is usually thought to depend only on soil type. However, as shown in Eq. 21, it is a function of the ratio between the pile impedance and the soil impedance for P-waves, that is, it also depends on the pile size and material. This fact, not generally recognized, is verified by a reanalysis of the vibration measurements reported by Heckman and Hagerty (1978), who measured the intensity of ground vibrations at different distances away from piles being driven. The piles were of different type, size, and material. Heckman and Hagerty (1978) determine the *k*-factor of Eq. 3 as a function of pile impedance and measurements of peak particle vibration velocity. The results are shown in Fig. 10a. [The one deviating point located away from the average curve through the other data points was obtained at the surface of a dense rubble fill through which the pile was driven using a follower, the impedance of which is not known].

The measurements were taken at different horizontal distances from different types and sizes of piles driven with hammers of different rated energies. Unfortunately, Heckman and Hagerty (1978) is somewhat short on details regarding the driving method, ground conditions, and vibration measurements. As shown in the figure, there is a strong correlation between the pile impedance and the *k*-factor, despite that the data also include effects of ground vibration attenuation and possibly effects of vibration amplification in soil layers. It can be seen that ground vibrations increased markedly when the impedance of the pile decreased. In fact, ground vibrations can be ten times larger in the case of a pile with low impedance, as opposed to vibrations generated at the same distance from the driving of a pile with high impedance (Massarsch 1992).

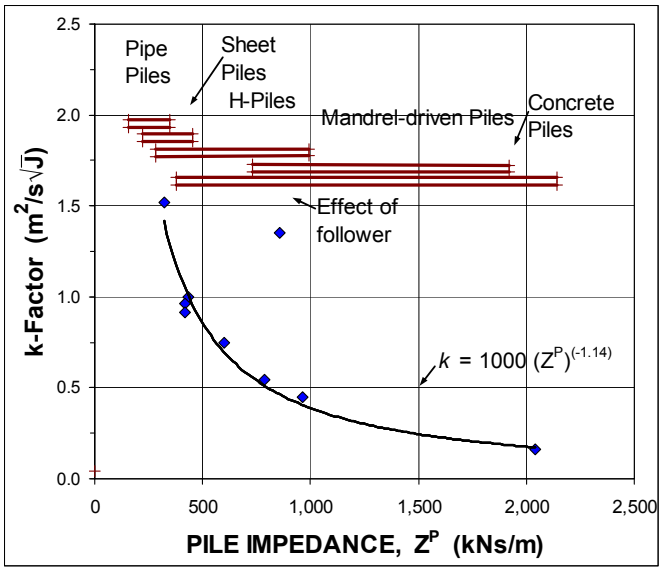

Fig. 10a. Influence of pile impedance on the vibration factor, k (Eq. 3). (Data from Heckman and Hagerty 1978).

Considering the implications of Eqs. 19 and 25, which show that vibration transmission efficacy is inversely proportional to the pile impedance, the data from Fig. 10a have been replotted in Fig. 10b to show the linear correlation between the *k*-factor and the inverse of the pile impedance.

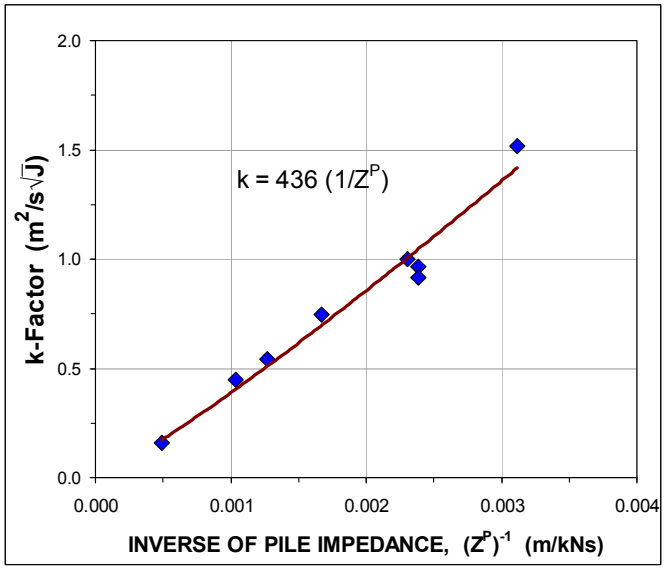

Fig. 10b. Relationship between K-factor and inverse of pile impedance, data from Fig. 10a replotted.

The correlation is surprisingly good, considering that the measurements were taken in different soil conditions and acknowledging the limitations of using the "*energy concept*" of Eq. 3. Indeed, the data reported by Heckman and Hagerty (1978) confirm that the energy transmission efficacy correctly reflects the vibration emission from the pile shaft and the pile toe to the surrounding soil layers. They also confirm the validity of the Eq. 21 and the fact, that the J_c-factor depends on the ratio between the soil and pile impedance values.

ENERGY PROPAGATION IN ELASTIC MEDIUM

The emission and propagation of vibrations from the pile to the surrounding soil layers is a complex process, as vibrations will be affected by the strain level. The vibration velocity is not directly proportional to strain. For example, wave velocity decreases more rapidly in granular soils than in clays at the same strain level. Vibrations are also affected by soil layering (resulting in refraction of wave rays), impedance difference between soil layers (causing partial reflection or refraction of vibration energy). Another potentially important aspect is vibration amplification due to resonance effects in soil layers. The below presented, simplified model can be used to calculate the propagation of different types of waves emitted from the pile shaft (cylindrical waves) and at the pile toe (spherical waves). In the future, it would be possible to develop a more sophisticated soil model using more advanced numerical methods. However, it is believed that simplifications will facilitate the understanding of the problem and that the present model captures the most important aspects of ground vibrations induced by pile driving.

Wave Attenuation in Elastic Medium

The transmission of vibrations can be analyzed based on theoretical considerations of energy propagation in an elastic medium (Clough and Penzien 1975). The energy source is assumed to be located in a homogeneous, isotropic elastic material. The vibrations generated by pile driving can be generated by strain energy, W_e and kinetic energy (of the accelerated mass), W_k, which both are a function of time, density (mass) and velocity, as shown in Eqs. 26 and 27.

$$W_e(t) = 0.5\,\rho\,v^2(t) \qquad (26)$$

$$W_k(t) = 0.5\,\rho\,v^2(t) \qquad (27)$$

where ρ = material density of soil
$v(t) = v_0 \sin(\omega t)$

As can be see, the maximum value of the strain energy and kinetic energy are equal but vary with time, t. In a conservative system, the total energy, W_0, is constant and the principle of conservation of energy applies, as expressed in Eq. 28.

$$W_0 = W_e(t) + W_k(t) = \rho\, v^2(t) \tag{28}$$

For the case of pile vibrations, two types of energy sources are considered, a spherical source and a cylindrical source, respectively. Based on elasticity theory, the particle velocity at any distance can be determined as a function of the released energy. It can be shown that the particle velocity also depends on the wave length, λ, of the propagating wave, which can be determined from Eq. 29.

$$\lambda = \frac{c}{f} \tag{29}$$

where λ = wave length
c = wave propagation velocity
f = frequency of vibration

Appendix A gives the derivation of expressions for vibration velocity (Eqs. A16 and A20) as function of energy at the vibration source and distance from the affected point and the source. Table 9 summarizes the theoretically derived equations and parameters needed for calculating vibration attenuation.

The distances, r_S and r_C, should be distance to the source of the vibration, as illustrated in Fig. 11 for spherical, and cylindrical waves. Note that the direction of vibration amplitude of the spherical wave is in the radial direction from the source, while that of the cylindrical wave is in the perpendicular (vertical) direction.

Table 9. Wave Attenuation Equations for Spherical and Cylindrical Waves, cf. Appendix A

	Spherical Wave (Eq. A14)	Cylindrical Wave (Eq. A16)
Particle Velocity, v(m/s)	$v_S = \frac{1}{(2\pi\rho\lambda)^{0.5}} \frac{(W_0)^{0.5}}{r_S}$	$v_C = \frac{1}{(\pi\rho\lambda h)^{0.5}} \frac{(W_0)^{0.5}}{(r_C)^{0.5}}$
k-factor	$k_S = \frac{1}{(2\pi\rho\lambda)^{0.5}}$	$k_C = \frac{1}{(\pi\rho\lambda h)^{0.5}}$
Units of *k*-factor	$\sqrt{\frac{m^2}{kg}}$	$\sqrt{\frac{m}{kg}}$

where v_S = particle velocity at point of measurement (m/s) of the spherical wave
v_C = particle velocity at point of measurement (m/s) of the cylindrical wave
W_0 = energy of wave at source (hammer) (J)
ρ = material density (kg/m^3)
r_S = distance between vibration source and measuring point for spherical wave (m)
r_C = horizontal distance from vibration source to measuring point for cylindrical wave (m)
k_S = material coefficient (m^2/kg)$^{0.5}$
k_C = material coefficient (m/kg)$^{0.5}$
λ = wave length (m) according to Eq. 29.
h_C = height of cylinder of propagating wave energy

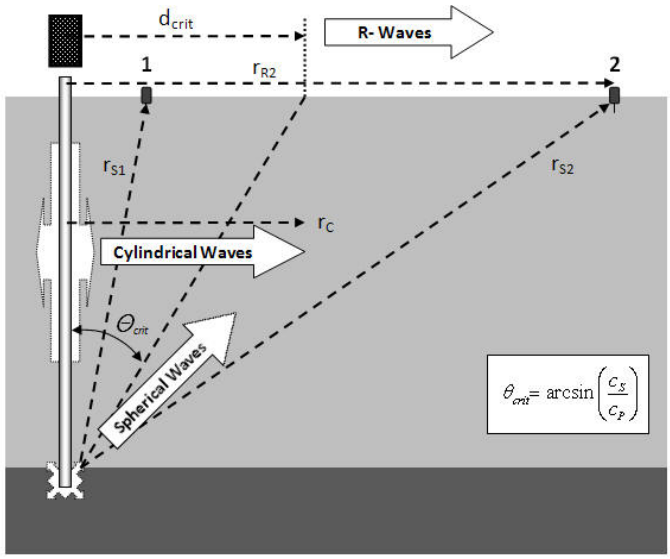

Fig. 11. Illustration of vibrations emitted during pile driving at the pile toe and along the pile shaft; c_S = shear wave velocity in the soil; c_P = stress wave velocity in the soil. d_{crit} = critical distance from pile.

Fig. 12 shows the relationship between the *k*-factors according to Table 9 and wave lengths for spherical and cylindrical waves. The *k*-factors for spherical waves and cylindrical waves bracket the empirical range of values shown in Fig. 4. For the case of cylindrical waves, different intervals of cylinder heights have been chosen, within a range covering the respective wave length (it is reasonable to assume that the wave length is approximately of the same magnitude as the cylinder height). The *k*-factors for the cylindrical waves are smaller than those of the spherical waves, cf. Table 9. However, the attenuation of particle velocity also depends on the distance r_S and r_C, (different values of exponent, 1.0 and 0.5, respectively). It should also be pointed out that the units of the *k*-factors are different for spherical and cylindrical waves. The two are therefore not directly comparable. This fact emphasizes the limitations of using Eqs. 3 or 4.

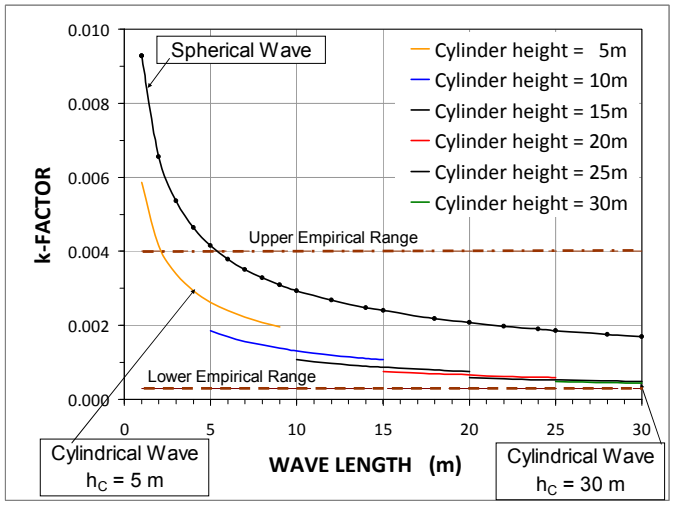

Fig. 12. Variation of k-factor (Eq. 3) as function of wave length according to Table 9 for a spherical wave and cylinder waves with height ranging from 5 m through 30 m. Soil density is 1,800 kg/m^3. Upper and Lower Empirical Range according to Fig. 4.

Reflection of Spherical Waves

When spherical waves, such as those emitted from the pile toe, encounter a free surface (ground surface), the waves are reflected or refracted as illustrated in Fig. 11. The reflection and refraction of waves depend on the angle of incidence, Θ. The analysis of waves which are reflected at a free surface is a complex task. However, it is possible to study a simplified case, that of an impinging P-wave (which is the dominant wave emitted from the pile toe) at the free surface for which the amplification factor, F_v, in the vertical direction, and the amplification factor, F_h, in the horizontal direction can be calculated from Eqs. 30a and 30b (Bodare 2005).

$$F_v = 2\frac{\cos\theta_P \cos 2\theta_S}{s^2 \sin 2\theta_P \sin 2\theta_S + \cos^2 2\theta_S} \qquad (30a)$$

$$F_h = 2\frac{\cos\theta_P \sin 2\theta_S}{s^2 \sin 2\theta_P \sin 2\theta_S + \cos^2 2\theta_S} \qquad (30b)$$

where Θ_P = angle of incidence of P-wave (cylindrical)
Θ_S = angle of incidence of S-wave (spherical)
s = ratio of sinus for angles of incidence of the *P*-wave and the *S*-wave
F_v = amplification factor vertical direction
F_h = amplification factor horizontal direction

The angles of incidence, Θ are measured to the vertical. The ratio between the angles of incidence of the *P*-wave and *S*-wave is conveniently expressed by s, which depends on Poisson's ratio, ν, according to the relationship in Eq. 31.

$$s = \frac{\sin\Theta_S}{\sin\Theta_P} = \sqrt{\frac{1-2\nu}{2(1-\nu)}} \qquad (31)$$

The amplification factor F_v *and* F_h according to Eqs. 30a and 30b are shown in Figs. 13a and 13b for different values of Poisson's ratio, ν, and angles of incidence.

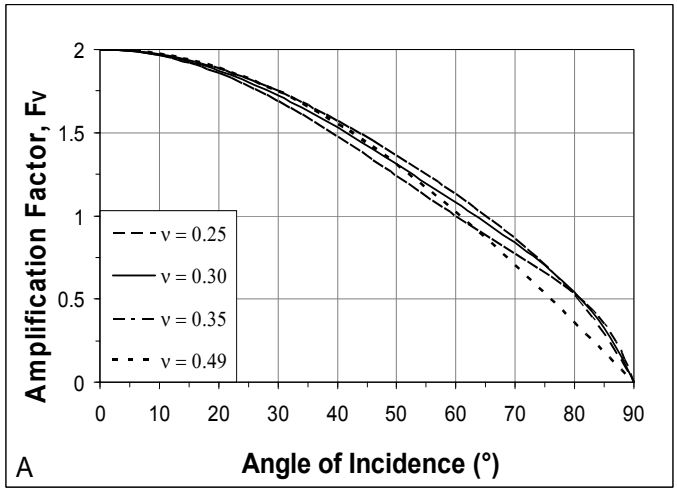

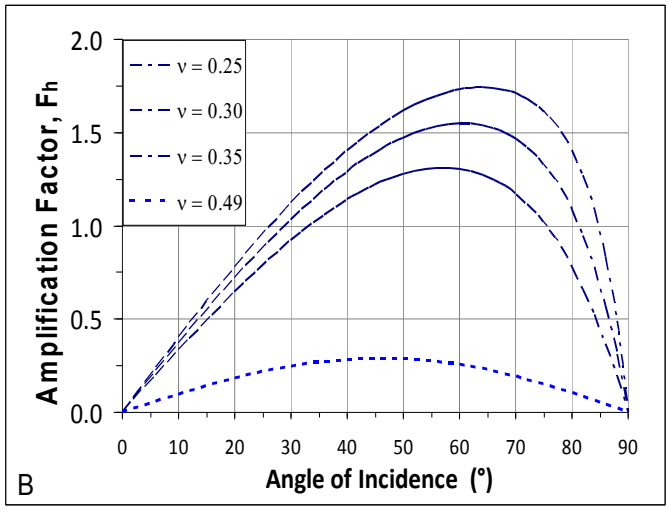

Fig. 13. Variation of vibration amplification factor at free surface of impinging P-wave for different values of Poisson's ratio.

It is apparent that the vertical vibration amplification factor is not strongly affected by Poisson's ratio. However, in the case of the horizontal vibration amplitude, a significant difference is obtained for horizontal amplification factors in granular (small Poisson's ratios) and fine-grained soils (large Poisson's ratios), respectively. For clays with a Poisson's ratio of 0.50, the amplification effect due to the incidence angle can be disregarded. This is not the case for granular soils with Poisson's ratio ranging typically between 0.25 and 0.35.

Directly above the source, the vibration amplitude of a vertically propagating P-wave (angle of incidence equal to 0^o) will double, ($F_v = 2$). At an angle of about 55 to 65 degrees, the amplification effect has vanished ($F_v \approx 1$). In most practical cases, P-waves will be of importance within a radius corresponding to one to two pile lengths, within which F_v varies between 2 and 1. At larger distances, the significance of the vertical amplitude gradually disappears. No amplification occurs directly above the vibration source in the horizontal direction ($F_h = 0$). However, at an incidence angle larger than 35 degrees, the vibration amplification effect should be taken into account.

Refraction of Spherical Waves at Ground Surface

Waves encountering a free surface can be reflected or refracted. Figure 11 indicates a distance called critical distance, d_{crit}, which is the distance from the pile to where a spherical wave (P-wave) emitted from the pile toe refracts as a surface wave on reaching the ground surface, also called Rayleigh wave (R wave). (The term R-wave is being used here to avoid confusion with shear waves—S waves). The angle Θ_{crit} denotes the angle of incidence of the wave which can be determined from Eq. 32 (Bodare 1997).

$$\Theta_{crit} = \arcsin\left(\frac{c_S}{c_P}\right) \qquad (32)$$

where c_P = P -wave velocity
c_S = S-wave velocity

It is now possible to estimate the critical distance, r_{crit}, from the pile at which wave refraction will occur at the ground surface (i.e. where surface waves will be generated), as indicated by Eq. 33.

$$r_{crit} = \tan\Theta_{crit} D \qquad (33)$$

where D = pile penetration depth
r_{crit} = critical distance from pile at ground surface at which surface waves are generated

Typical values of the critical distance are given in Table 10 for different values of Poisson's ratio. The table suggests that in dry coarse-grained soil (Poisson's ratio between 0.20 – 0.35), the critical distance from the pile, r_{crit}, is located at a distance approximately equal to half the embedment depth of the pile, D. In loose or soft soils below the groundwater level, the critical distance becomes much shorter and is in the case of clay almost zero.

The procedure expressed in Eqs. 30a and 30b of determining the R-wave amplification factor is a powerful approach which is not widely used in pile driving practice, but it is well-known in soil dynamics.

Table 10. Ratio of Critical Distance, d_{crit} to pile penetration depth D at which R-waves are emitted (Eq. 32), cf. Fig. 11

Poisson's ratio, v	Θ_{crit} degrees	r_{crit}/D
0.20	28	0.53
0.25	25	0.46
0.30	21	0.39
0.35	18	0.32
0.40	14	0.25
0.49	4	0.07

Propagation of Surface Waves

Surface (R-) waves, which are generated by refracted P- and S-waves at the free surface, attenuate along the ground surface according to Eq. 34 (Massarsch 1992).

$$A_2 = A_1\left(\frac{R_2}{R_1}\right)^{-n} e^{-\alpha(R_2 - R_1)} \qquad (34)$$

where A_1 = vibration amplitude at distance R_1 from source
A_2 = vibration amplitude at distance R_2 from source
α = absorption coefficient

For surface waves, the exponent n is equal to 0.5. Equation 34 is shown in Fig. 14. Note that in the vicinity of the pile, shear strain levels can be larger and reduce wave velocities; this effect should be taken into consideration in a detailed analysis.

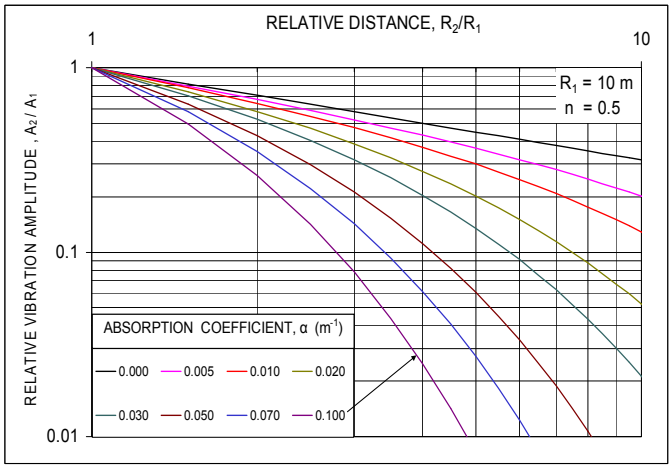

Fig. 14. Attenuation of surface waves (n = 0.5): relative amplitude, A_2/A_1, as a function of relative distance, R_2 R_1, for a range of absorption coefficients (R_1 = 10 m). cf. Fig 15.

It is important to appreciate that the absorption coefficient, α, is not a material-independent constant, as often assumed, but one that varies with vibration frequency and wave propagation velocity (and thus also indirectly with shear strain). The absorption coefficient, α, is of importance for the vibration attenuation, as can be estimated from the Eq. 35 (Massarsch 1992).

$$\alpha = \frac{2\pi\, D_M\, f}{c_R} \tag{35}$$

where α = absorption coefficient (m^{-1})
D_M = material damping $(Hz\ s)^{-1}$
f = vibration frequency (Hz)
c_R = surface wave velocity (m/s)

For elastic waves (at a distance of at least one wave length), the material damping can be assumed to be within the range of 3 to 5 %.

The surface wave velocity is for most practical purposes the same as that of the shear wave velocity. The variation of the absorption coefficient is shown in Fig. 15 as a function of the wave velocity and for different values of vibration frequency.

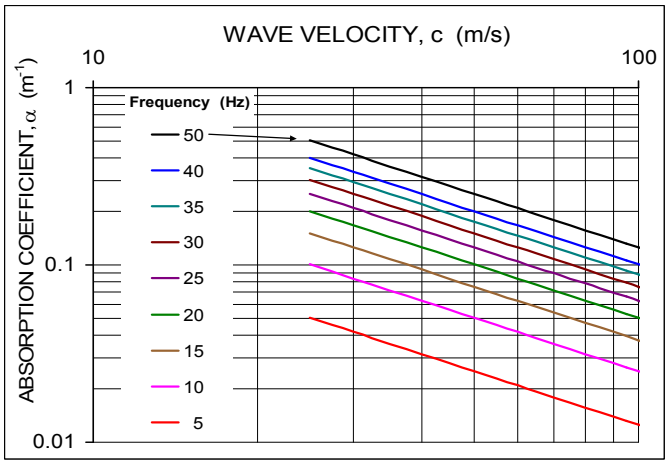

Fig. 15. Absorption coefficient α as function of wave velocity for different vibration frequencies (the assumed value of material damping is 4 %).

CALCULATION OF GROUND VIBRATIONS

The concept of calculating ground vibrations induced by pile driving is based on the following approach:

- Determine the dynamic pile hammer properties
- Determine the dynamic pile properties
- Estimate the peak particle velocity of the stress wave
- Assess the vibration transmission efficacy along the pile shaft and at the pile toe
- Calculate the propagation of spherical wave energy from the pile toe to the ground surface, taking into account wave reflection
- At the critical distance from the pile on the ground surface, calculate the vibration attenuation of surface waves
- Calculate the f cylindrical waves from the pile shaft.

The calculation method of ground vibrations due to spherical waves, surface waves and cylindrical waves is explained below. As has been pointed out earlier in this paper, all three waves can occur at the same time and their intensity will depend on the driving method and vary with respect to the dynamic soil resistance along the pile shaft and at the pile toe.

Spherical Waves

Spherical waves are caused by the dynamic resistance at the pile toe. Assuming only P-waves is a simplification of the real situation, but makes it possible to capture the most important aspects of vibration transmission. The attenuation of vibration velocity emitted from the pile toe can be calculated based on Eq. A14 as given in Table 9. Note that the vibration amplitude is taken in the radial direction from the pile toe.

The vibration transmission factor at the pile toe, E_T, defines the maximum vibration velocity that can be transmitted to the soil at the toe, as well as the hammer efficiency factor, F^H, takes into account the loss of impact energy from the hammer to the pile head. The amplification effect due to vertical reflection of vertical vibration amplitudes at the ground surface is accounted for by F_v, considering also the angle of incidence of the emitted wave at the ground surface Θ.

The vertical ground vibration velocity, v_{Sv}, due to spherical (body) waves emitted from the pile toe can now readily be determined from Eq. 36.

$$v_{Sv} = k_s F_v E_T \frac{(F^H W_0)^{0.5}}{r_r} \cos\Theta \tag{36}$$

where v_{Sv} = vertical component of spherical wave amplitude
k_S = vibration factor for spherical waves (Table 9)
F_v = vibration amplification factor (Eq. 9a)
E_T = vibration transmission efficacy at pile toe (Eq. 25)
F^H = hammer efficiency factor (Table 7)
W_0 = potential energy generated of pile hammer
Θ = angle of incidence of spherical wave at ground surface
r_r = radial distance to the pile toe

Cylindrical Waves

Cylindrical waves are emitted from that part of the pile shaft where the stress wave is in contact with the surrounding soil. (It is appreciated that other types of waves can be emitted along the pile shaft and in other directions, but these are neglected in the case of impact pile driving). It is assumed that the cylindrical waves propagate horizontally from the pile shaft. Their vertical vibration amplitude and the rate of vibration attenuation are similar to that of surface waves. The vertical vibration velocity at the ground surface can be determined based on Eq. A16 given in Table 9. The vibration transmission efficacy, E_S, defines the maximum vibration velocity that can be transmitted to the soil along the shaft. The hammer efficiency factor (or ratio), F^H, takes into account the loss in impact (kinetic) energy. The velocity of the vertical ground vibration, v_C, due to cylindrical (shear) waves emitted along part of the pile shaft (which depends on the wave length of the stress wave) can now readily be determined from Eq. 37.

$$v_c = k_c E_S \frac{(F^H W_0)^{0.5}}{(r_c)^{0.5}} \tag{37}$$

where v_C = vertical component of cylindrical wave amplitude
k_c = vibration factor for spherical waves (Table 9)
E_S = vibration transmission efficacy along pile shaft (Eq. 19)
F^H = hammer efficiency factor (Table 7)
W_0 = potential energy of pile hammer
r_C = horizontal distance from the pile shaft

Surface Waves

Surface waves are caused by refraction of P- and S-waves at the ground surface at the critical distance, r_{crit}, which can be determined from Eq. 33. The vertical vibration amplitude is determined according to Eq. 36 and vibration attenuation can then be calculated with input of Eqs. 34 and 35. Note that a spherical wave emitted from the pile toe can reach a measuring point both directly and as a refracted surface wave. However, the spherical wave attenuates more rapidly and has little practical consequences beyond a horizontal distance from the source equal to about 2 pile-embedment depths, i.e., corresponding to a 2(H):1(v) distance ratio.

Equations 36 and 37 express the vertical vibration velocity generated at a point from a pile driven at a certain distance away. As such, they, combined with Eqs. 19 and 25, allow a rational analysis of the effect of driving piles near a vibration susceptible structure and allow the potential disturbance to be estimated prior to construction start. The horizontal component of ground vibrations of R-waves can be readily determined for different soil types (Poisson's ratio) and solutions are available in the literature (Richart et al. 1970).

It should be mentioned that the emission of vibrations from the pile shaft and the pile toe can occur at the same time and result in amplification of ground vibrations due to wave superposition. However, at this stage, and since the waves propagate at different velocities and over varying distances, this effect is neglected. The above outlined concept of calculating ground vibrations will now be applied to an analysis of field measurements from a well-documented case history.

CASE HISTORY OF PILE DRIVING VIBRATIONS

General Comments on Data from Case Histories

Most case histories reporting vibration measurements from pile driving contain insufficient information for a scientific analysis. Many — even peer reviewed papers and academic theses — lack basic information about the pile driving method (hammer and pile dynamic information), geotechnical site conditions (penetration tests) and dynamic soil properties, how the vibration measurements were performed, time histories and frequency content of vibrations, direction of measured amplitude (vertical or horizontal), definition of measured parameters (RMS values, peak or peak-to-peak values), depth of pile at the time of measurement, definition of distance (at ground surface or from pile toe), and interpretation of measurement results. Although simple records of the penetration resistance (blow-count) and a comparison with penetration test results can provide valuable information, it is rarely available. As has been demonstrated in this paper, also the geometric dimensions and dynamic properties of the pile hammer and of the pile constitute important information essential for the assessment of ground vibrations.

Case histories reporting ground vibration measurements should— as a minimum — contain the following information.

- the geotechnical site conditions (location of groundwater table and soil layering, preferably based on cone penetration test data)
- dynamic soil properties (shear wave velocities of soil layers — obtainable in a cone penetration test)
- details on the piles (geometry and material properties including impedance)
- pile driving equipment (type of hammer, ram travel or height-of-fall, and impedance of hammer)
- detailed description of pile installation process (penetration resistance records, depth of pile toe

at time of measurement), and detailed description of measuring equipment (type of sensors, direction of measurement, distance and direction)
- vibration measurements in at least two directions, preferably all three directions, at least at one reference location
- documentation of measured data (at least a few time history traces), preferably available also in digital format
- results of data analyses (frequency spectra).

With the availability of highly accurate sensors, powerful data acquisition systems, and efficient analytical tools, it should no longer be difficult to collect and interpret even large quantities of measurement data – even in real time. This fact is illustrated by the widely used, and cost-effective application of stress-wave measurements for obtaining driving records and bearing capacity analysis. In this context, it is surprising that in the past, pile dynamic measurements have focused exclusively on the determination of penetration resistance and pile bearing capacity, completely neglecting the wealth of information that stress-wave measurements can provide for the evaluation of ground vibrations.

Site Conditions and Measurement Arrangement at Test Site

The authors have had access to comprehensive field tests published by Nilsson (1989), describing vibration measurements during the driving of a series of test piles. The main objective was to establish site-specific driving methods and to select the optimal pile type which would minimize ground vibrations. Ground vibrations were of major concern due to the fact that several buildings and installations in the vicinity were susceptible to vibrations. Although the reported data are not complete (stress-wave measurements were carried out, but data were not available), they offer the possibility of analyzing the field data and to compare these with the theoretical concepts proposed in this paper.

The field tests were performed in the southern part of Sweden near the city of Skövde. In this area, located inland, the soil conditions are somewhat different to the well-known, soft clay deposits in the coastal regions. The soil profile in the test area was about 2 m to 4 m of surface fill, consisting of well-compacted, alternating layers of furnace slag sand-size particles and sand and gravel. Below followed a relatively homogeneous, 12 m thick layer of medium stiff clay with average undrained shear strength of 30 kPa deposited on a layer of sand with a thickness of 7 m on glacial till. Bedrock was encountered at a depth of about 25 m below the ground surface. The groundwater table was located about 3 to 4 m below the ground surface at the top of the clay layer. Unfortunately, data from more detailed geotechnical investigations (such as penetration tests or soil sampling) are not available. The geotechnical properties (with interpreted values) of the soil layers are summarized in Table 11.

Table 11. Geotechnical soil profile at test site

Soil	Layer Thick-ness (m)	Stiffness/ Strength (kPa)	Density (kg/m^3)	Shear wave velocity m/s*)	Poisson ratio
Fill of slag and sand	3	-	1,900	150 – 200	0.3
Clay	12	30	1,600	100 – 150	0.5
Sand and gravel	7	loose to dense	1,800	250 – 350	0.3
Glacial till	3	stiff	1,900	400 – 600	0.3

*) Assumed

Test Pile

The existence of a stiff surface layer on top of the clay indicated that vibration problems would likely occur during the beginning of the driving. Vibration problems could also be expected during seating of the piles into the bearing layer at 24 to 25 m depth. Allowable vibration values with respect to damage to the existing structures and installations were estimated according to Swedish standard SS 02 52 11 (SIS 1999). As the piles were driven into sandy, clayey soils, the standard indicated a vibration velocity, v_0, equal to 9 mm/s (Table 1). The buildings were of normal type ($F_b = 1$), constructed of reinforced concrete ($F_m = 1.2$), and with foundations on toe-bearing piles ($F_g = 1.0$). Therefore, according to Eq. 1, the maximum allowable vibration velocity (vertical component) was $v_{max} = 10.8$ mm/s. A separate study regarding the environmental effects of pile driving (noise and vibrations) on occupants of buildings and installations was performed, but is not addressed in this paper.

In order to assess the effect of ground vibrations at the site from driving different pile types, a series of piles were installed and extensive vibration measurements were performed (Nilsson, 1989). The present paper is limited to the results of driving one test pile, a reinforced concrete pile with a square cross section (270 x 270 mm). The concrete pile has a wave velocity of 4,000 m/s, a bulk density of 2,400 kg/m^3, and a cross section area of 0.0729 m^2, which corresponds to a

pile impedance, Z^P, of 714 kNs/m. The pile was made up by three segments of lengths (13.3 + 10 + 6 = 29.3 m), which were jointed in the field with a mechanical type splice. The test pile was driven by a hydraulic hammer type Banut with a ram mass of 4,000 kg and a length, L^H, of 3.65 m.

During the driving through the overburden soils, the hammer height-of-fall was kept to 0.40 m. It was increased to 0.50 m during the termination driving into the stiff glacial till at a final depth of approximately 25 m. Figure 16 shows the pile driving diagram, where the number of blows per 0.5 m is plotted as well as the accumulated number of blows. Also shown are the soil layers described in Table 11, as well as the depths where vibration measurements were performed.

Vibration Measurements

Vibration measurements were performed using five geophones of type SM-6/9 (three gages measuring vertical vibration, i.e., particle velocity, and two gages measuring horizontal vibration). The "vertical" geophones were placed at 10 (V1), 20 (V2) and 40 m (V3) distance from the test pile, Fig. 17. A data logger recorded the peak value of vibration velocity at each hammer blow as well as the depth of the pile at each measurement. At a horizontal distance of 20 m, vibrations were also measured horizontally in the radial (H4) and transverse (H5) directions of wave propagation. The signals were amplified and registered by a tape recorder, stored digitally, and later analyzed.

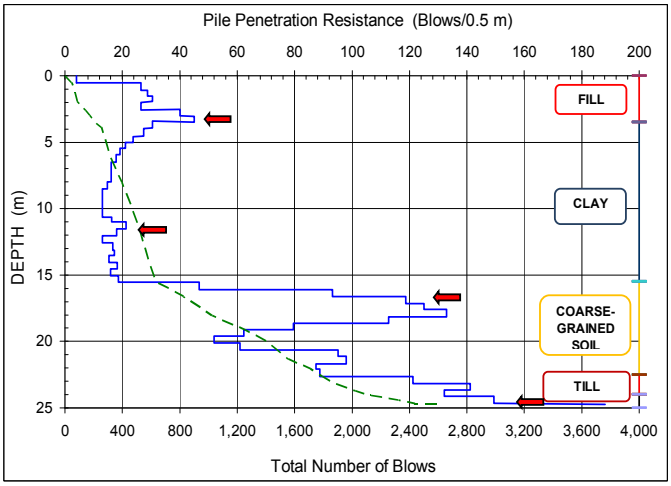

Fig. 16. Penetration resistance during driving of 29 m long concrete pile with hydraulic hammer to 25 m depth. Also indicated are main soil layers and by arrows the depths at which detailed vibration analyses were carried out.

At 20 m horizontal distance from the pile, ground vibrations were measured in three directions, during penetration of the pile and termination driving at 25 m depth. Since all three vibration components are known, it is possible to determine the resultant of vibration amplitudes. It should be noted that the resultant amplitude was calculated from the maximum (peak) values in three directions, and may therefore slightly overestimate the actual maximum amplitude (the maximum may not necessarily have occurred at the same time in all three directions). The 40-m measuring point is 1.6 pile lengths horizontal distance away from the pile and 1.9 pile lengths distance away from the pile toe at end of driving. Because the vibration measurements were made simultaneously in both radial and vertical directions, it is possible to determine also the inclination of the resultant vibration amplitude in the direction of wave propagation, as indicated in Fig. 18. Also shown in the figure is the calculated inclination of waves which, theoretically, would be emitted from the pile toe only—assuming linear wave paths.

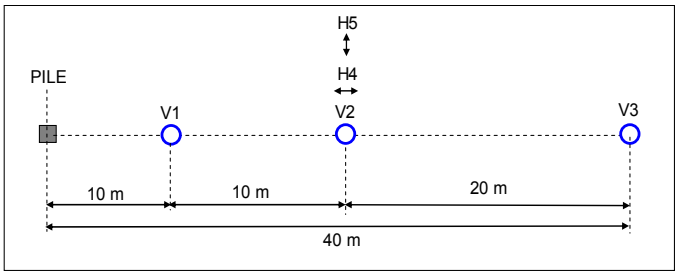

Fig. 17. Arrangement of vibration sensors during driving of the test pile. V1, V2, and V3 indicate "vertical" and H4 and H5 indicate "horizontal" geophones.

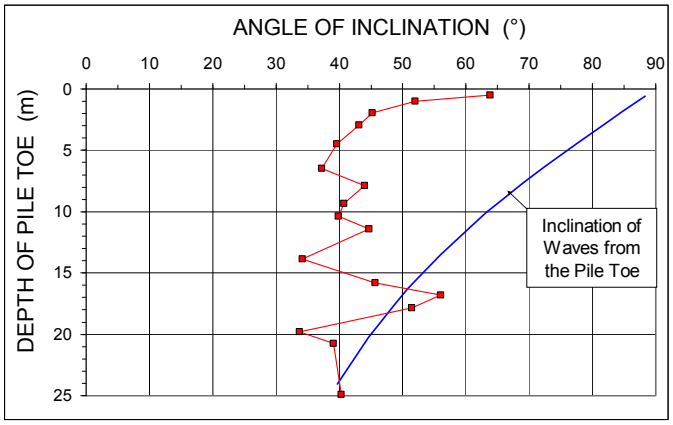

Fig. 18. Inclination of resultant vibration amplitude (as angle to the vertical) and estimated angle of incidence of waves emitted from pile toe. Note that a low angle of inclination implies a larger vertical vibration amplitude.

The inclination of vibration amplitudes during pile driving through the surface fill and clay layer is clearly lower than the inclination if vibrations would have been emitted from the pile toe only. Therefore, in these layers, it can be concluded that a large part of vibration energy occurs at, and is transmitted along the pile shaft and/or propagate as surface waves.

However, when the pile toe encountered the dense glacial till at 17 m depth, the measured inclination of vibration amplitude (horizontal component) increases and vibrations agree best with those emitted as spherical waves from the pile toe.

Based on these simple vibration measurements it is possible to estimate the likely origin of the ground vibrations during pile penetration into different soil layers at a distance of 20 m. Above 17 m depth, a large part of ground vibration energy is emitted in the form of cylindrical waves (or surfaces waves at later distance) while below 17 m, most vibrations are emitted from the pile toe. Note that the interpretation of ground vibration amplitudes depends on the relative distance between the pile and the point of observation, as illustrated in Fig. 2. Of course, a more detailed analysis of pile resistance distribution would be possible from analysis of stress-wave measurements. Nevertheless, even the simple vibration measurements results reported here provide valuable insight into the pattern of vibration propagation.

The vertical vibration velocity was measured at three distances from the pile and the results are shown in Fig. 19.

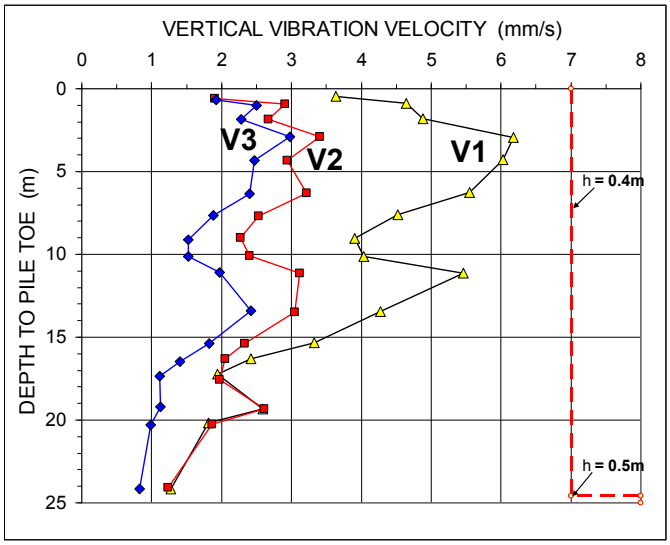

Fig. 19. Vertical vibration velocity at three distances as function of pile depth together with the hammer height-of-fall.

When the pile was driven through the surface fill, the magnitude of the vibration amplitudes at 10 and 20 m distance are relatively equal, compared to that at 40 m distance. The vertical vibration velocity decreases markedly with increasing horizontal distance to the pile. This observation reinforces the previously mentioned observation that cylindrical waves (or surface waves) dominate during pile driving through the upper soil layers. However, when the pile toe encounters stiff soil layers, spherical waves begin to dominate. At a pile depth range of 17 to 25 m, the direct distance from the pile toe to the measurement points V1 and V2 are 26 m and 32 m, respectively (small difference in terms of vibration propagation), which explains why the measured vibration amplitudes are almost the same.

During the driving of the pile, vibration records in the time domain (vibration time histories) were obtained at several distances and these records were also analyzed in the frequency domain (as Fourier spectra). Figures 20 through 23 show the time histories of vibration records at 10, 20 and 40 m from the pile at a toe penetration depth of 3 m. The time of hammer impact is also indicated. The dominant vibration frequency is for all three locations in the range of 8 through 15 Hz, with a similar distribution of the frequency content at all measurement locations. The dominant (central) frequency is found at 13 Hz. It is of interest to investigate the difference in frequency content at one location between the vertical, the radial, and transversal vibration amplitude.

There is a distinct difference between the frequency spectra of the vertical, radial, and transversal vibration amplitudes. While in the case of vertical vibrations, there appears to be one dominant frequency range (about 13 Hz), the frequency spectra of the horizontal records are much broader, with dominant frequency peaks at 45 Hz. This underscores the assumption that horizontal vibrations are due to P-waves, while vertical vibrations are caused by the cylindrically expanding wave front, which propagates at the velocity of shear waves. Figs. 22 and 23 compare the effect of soil resistance on ground vibrations in the vertical and radial direction. The time history traces are shown for three interesting depths, 11.5 m (where pile driving was halted to splice the pile), at 17 m depth (during penetration into the stiff layer of sand and gravel) and at 25 m depth (during end-of-driving).

When the driving was resumed at 11.5 m depth, the penetration resistance showed an increase relative the resistance before the pause. (It is well-known that piles driven in clay and left to rest, excess pore water pressure dissipates causing pile “set up”. The increased penetration resistance resulted in an increase of vibration velocity, as can be seen in Fig. 22 and Fig. 23, an effect which also is even more apparent in Fig. 19. The velocity decreased as the shaft resistance diminished in the continued driving.

At 17 m depth, the driving resistance increases sharply as the pile enters into the denser layer of sand and gravel. However, it is noted that the vertical ground vibrations did not increase correspondingly, while the horizontal vibration rose sharply.

During termination driving at 25 m depth (with hammer height-of-fall increased to 0.5 m), the width of dominant frequencies of the horizontal vibrations increased and covered a much wider range, while the dominant frequency of vertical vibrations remained low at around 10 Hz. The vertical and horizontal vibration amplitude were now almost equal.

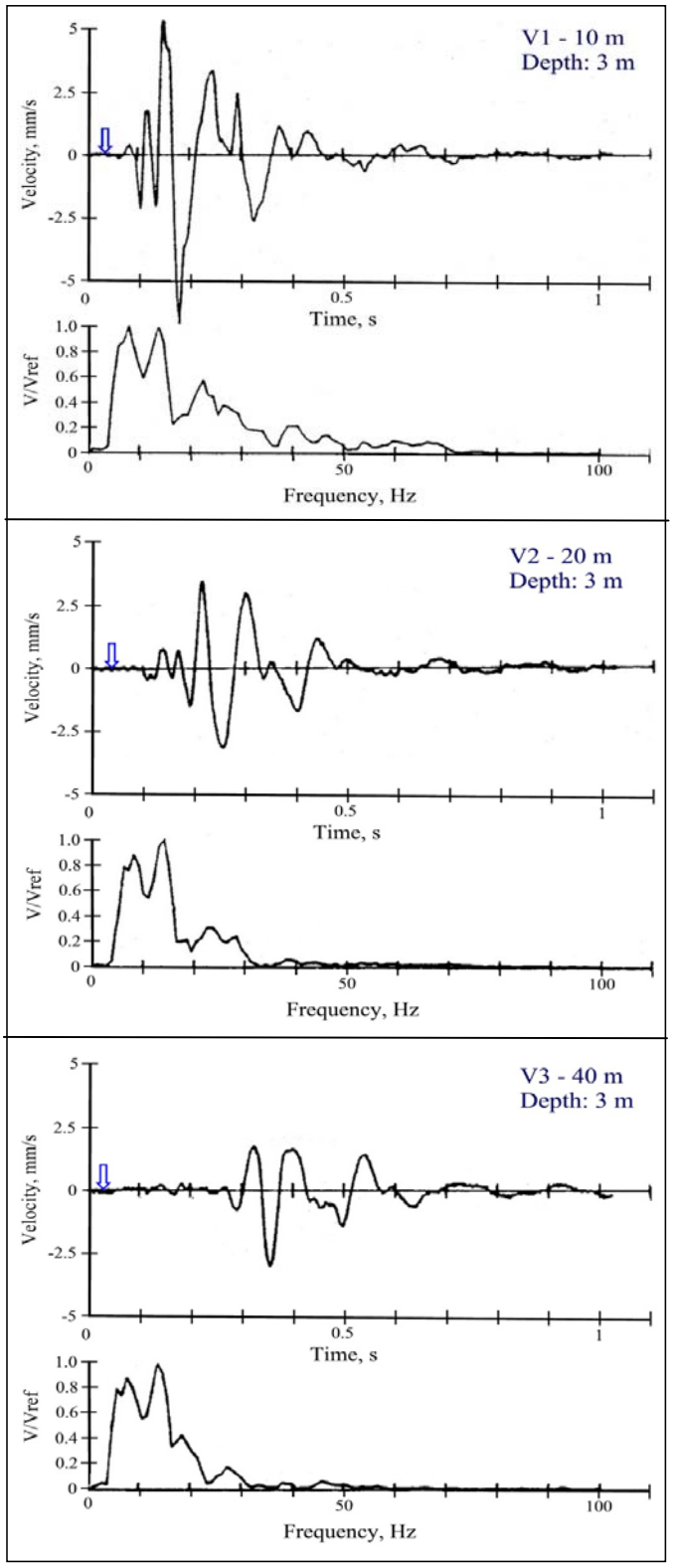

Fig. 20. Vertical vibration velocity records and normalized Fourier spectra for measurement locations V1, V2, and V3 during pile driving at 3 m depth. The arrow indicates the time of hammer impact.

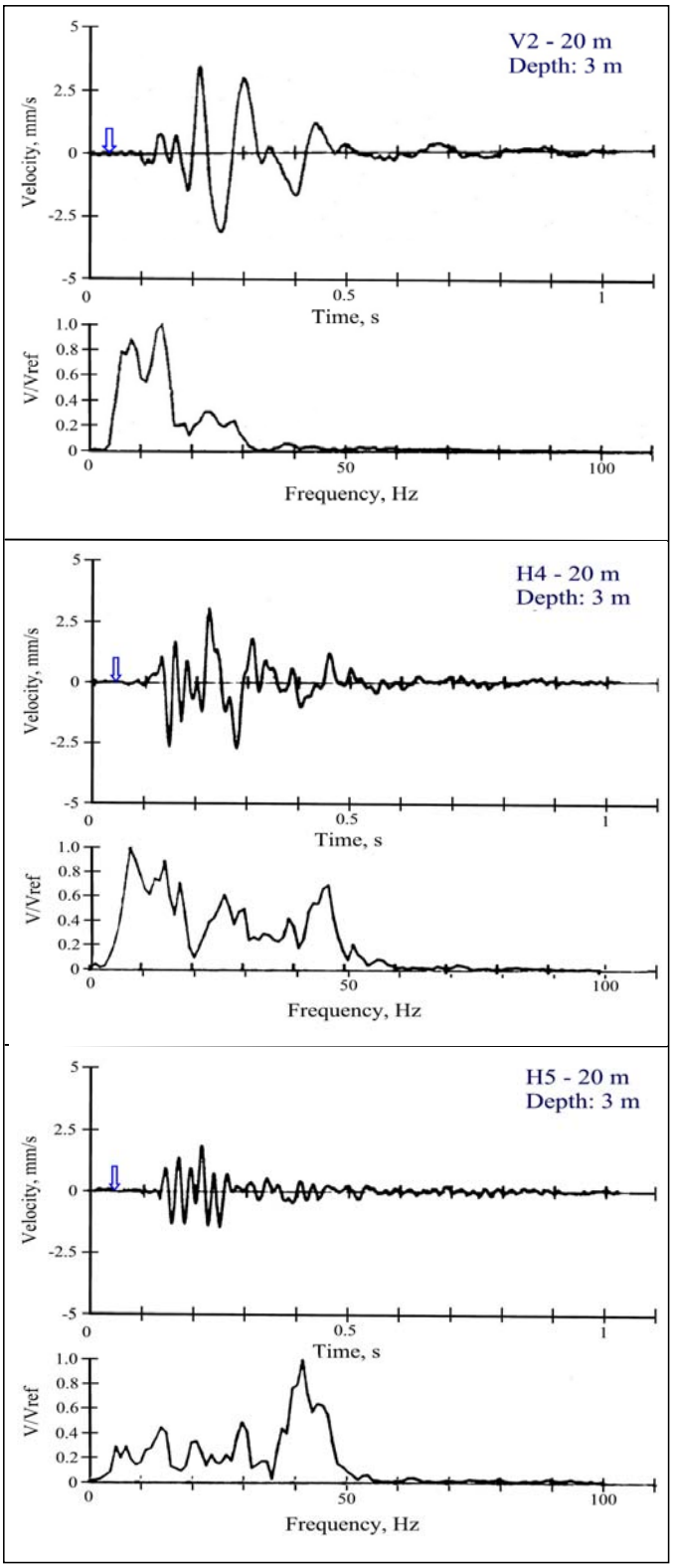

Fig. 21. Vibration velocity records and normalized Fourier spectra at 20 m distance for sensors V2 (vertical), H4 (radial) and H5 (transversal) during pile driving at 3 m depth. The arrow indicates the instant of hammer impact.

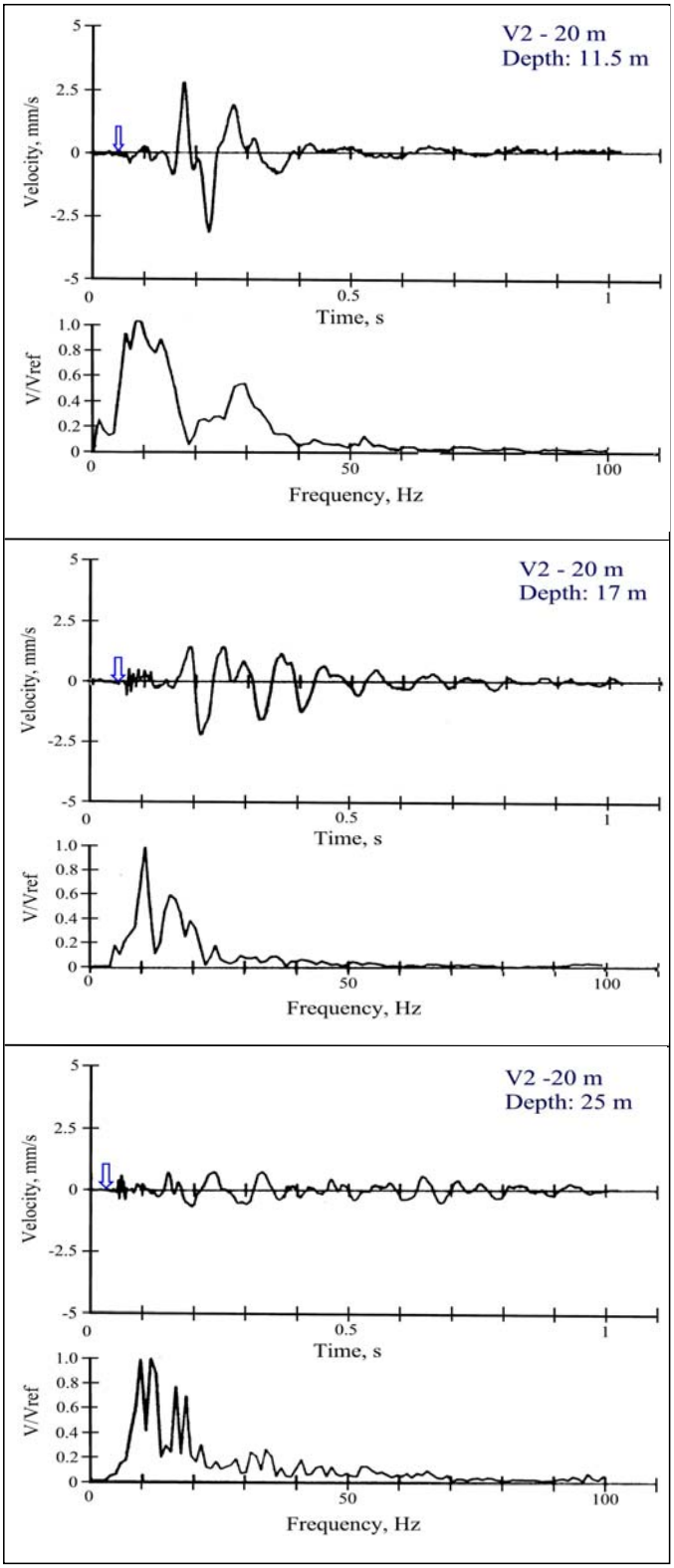

Fig. 22. Vertical vibration velocity records and normalized Fourier spectra for measurement location V2, during pile driving at 11.5, 17, and 25 m depth. The arrow indicates the time of hammer impact.

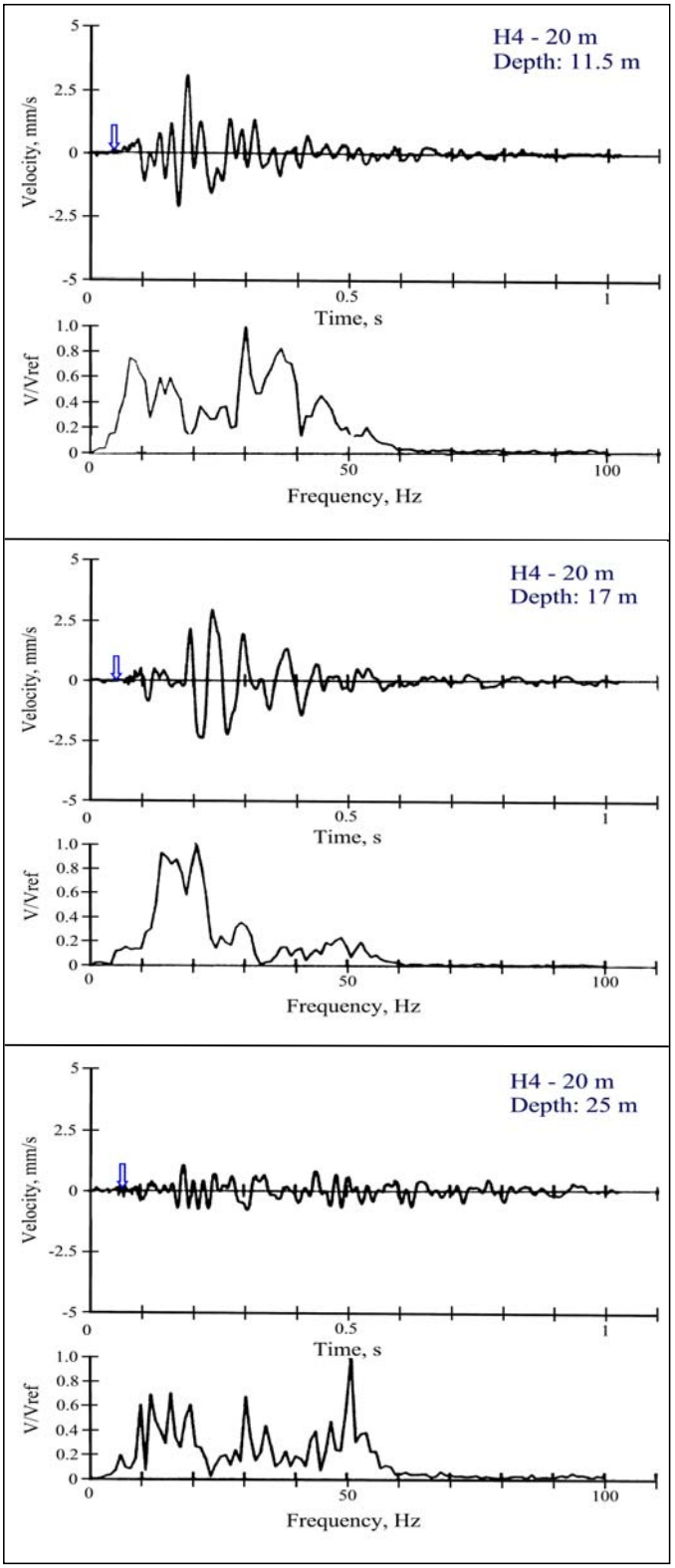

Fig. 23. Vertical vibration velocity records and normalized Fourier spectra for measurement location H4 (radial), during pile driving at 11.5, 17, and 25 m depth. The arrow indicates the time of hammer impact.

Vibration Velocities

From the records of vertical particle vibrations, the wave propagation velocities can be estimated since the time of hammer impact is known. Two methods were used to determine wave velocities: interval time from hammer impact to first peak, using horizontal propagation direction (cylindrical waves emitted from pile shaft) and interval time from hammer impact to first arrival (spherical waves emitted from pile toe). It is acknowledged that the method is crude, but it provides useful insight which wave velocity values should be used when analyzing pile vibrations. Figure 24 shows the calculated wave velocities determined from 0.5 m to 16 m depth, for which depth range most of the vibration energy propagated by cylindrical waves. This wave velocity was close to the average shear wave velocity of the soil layers of 125 through 175 m/s.

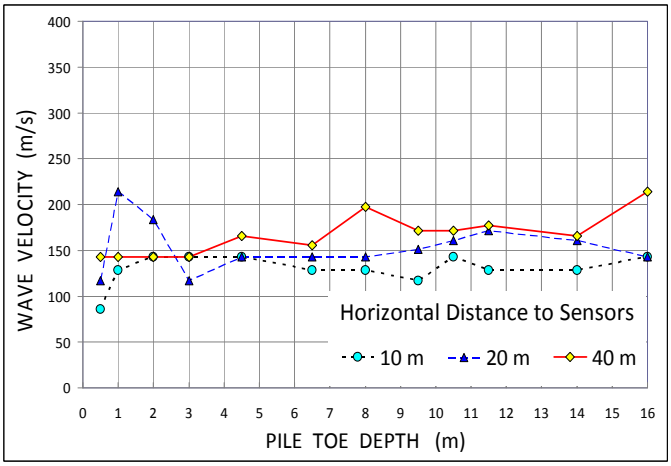

Fig. 24. Velocity of cylindrical wave, determined from first peak of velocity amplitude at sensors V1, V2, and V3, respectively, as measured at different pile toe depths.

For penetration depths from 17 to 25 m, wave velocities were determined from the time interval between hammer impact and first arrival of vibrations at the three sensor locations. The direct distance from the pile toe to the sensor locations on the ground surface were used to calculate the wave velocities, as presented in Fig. 25.

The highest velocities were measured at sensor location V1, where the waves were propagating at a steeper angle than at locations V2 and V3. Wave velocities increased with pile penetration depth, confirming that wave velocities increase in the stiffer bottom layers. Also the groundwater table will have affected the wave propagation velocity at steeper propagation angles. The wave velocities range from 425 m/s at V1 to 200 m/s at V3. The difference between wave velocities decreased at larger distances from the pile.

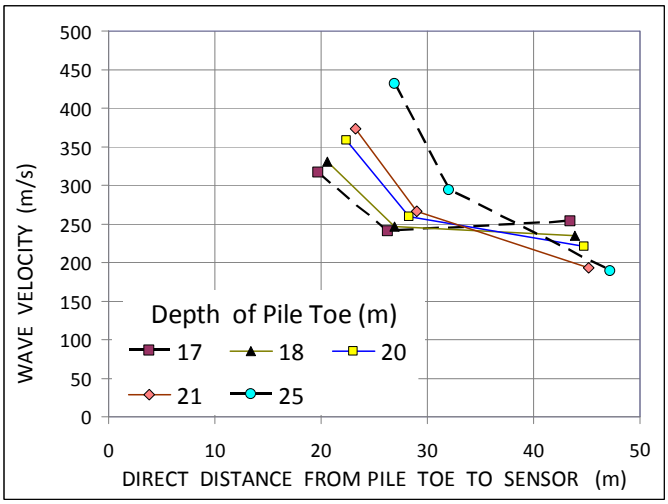

Fig. 25. Velocity of direct (spherical) wave determined from first arrival from pile toe to sensors V1, V2, and V3, respectively, as measured at different pile toe depths.

INTERPRETATION OF VIBRATION MEASUREMENTS

Unfortunately, the geotechnical information from the case history is not complete. In particular, results from penetration tests would have provided valuable information regarding soil stiffness and strength. However, based on the general soil profile and the penetration resistance from the test pile, it has been possible to compile representative geotechnical data for the analysis and compile typical values of soil data to establish a reference to the analysis method. The so-compiled soil data are summarized in Table 12 and were chosen based on the pile penetration resistance distribution shown in Fig. 16.

Table 12. Assumed geotechnical properties of soil layers

Soil Type	Layer Thick-ness (m)	Density (kg/m^3)	c_P (m/s)	c_S (m/s)	Poisson's Ratio	R_c
Sand fill	3.5	1,900	400	200	0.33	0.25
Clay	12.0	1,600	1,450	125	0.49	0.30
Sand gravel	7.0	1,800	1,450	300	0.33	0.30
Glacial till	1.5	1,900	1,450	500	0.33	0.35

Hammer and Pile Dynamic Data

An important factor affecting ground vibrations is the dynamic performance of the pile driving hammer. The test pile was driven by a hydraulic hammer of type Banut with properties given in Table 13, while the dynamic data for the pile are compiled in Table 14.

Table 13. Data for the Banut hydraulic hammer (i.e., ram)

Mass (kg)	4,000
Steel density (kg/m^3)	7,800
Velocity Steel, c^H (m/s)	5100
Hammer length, L^H (m)	3,65
Hammer Impedance (kNs/m)	27,200
Height-of-fall during driving (m)	0.4
Height-of-fall at end-of-driving (m)	0.5

Table 14. Pile Data.

Cross section area (m^2)	0.0729
Bulk density (kg/m^3)	2,400
Velocity, c^P (m/s)	4,000
Total Length, L^H (m)	29.3
Impedance (kNs/m)	714

The driving energy, W_0, can now be calculated, using a hammer efficiency factor of $F^H = 0.9$, which is a typical upper value for hydraulic hammers. Note that for the calculation of ground vibration, applying upper limits is a conservative approach.

Calculation of Spherical Waves Emitted from the Pile Toe

When the pile toe penetrates into a soil layer, vibrations are emitted in the form of spherical waves (mainly P-waves). The vertical vibration (mainly P-wave) amplitude was measured when the pile toe was at four depths (3.0, 11.5, 17.0, and 24 m) for the three vibration sensors at the horizontal distances, 10, 20 and 40 m from the pile. The calculation depths are indicated in the pile driving diagram, Fig. 16. As a first step, the incidence angle of the wave at the ground surface is calculated, assuming a straight ray path from the pile toe to the ground surface. The vibration amplification factor F_v can then be determined, assuming Poisson's ratio of 0.33. Next, the k_S-factor is calculated according to the equations presented in Table 9 (Eqs. A14 and A16).

The vibration transmission efficacy, E_T can be determined from Eq. 25. Below the groundwater table, the P-wave velocity, c_P, is assumed to correspond to that of saturated water (1,450 m/s) from which the corresponding specific soil impedance, z_P, is determined. Note, however, in coarse-grained soils, the P-wave velocity is likely to increase below the pile toe due to compaction and may be reduced in fine-grained soils due to disturbance and pore water pressure increase.

From Eq. 36 the vertical ground vibration velocity $v_{S,v}$ caused by emission of spherical waves, can be calculated at different radial distances from the pile toe, r_r taking into account the inclination of the incident wave, Θ.

The calculation steps of spherical waves emitted from the pile toe are summarized in Table 15. The vibration velocities determined in Table 15 are shown in Fig. 26 together with the measured vertical vibration velocities. The comparison between calculated and measured vibration velocities indicates that the waves emitted during the driving are not in the form of spherical waves (P-waves). The spherical waves—as expected—will not dominate until the pile penetrates into the stiff bottom layers (sandy gravel and moraine), and they have little significance when the pile penetrates the surface layer and the soft clay deposit.

Table 15. Calculation of Spherical Waves (P-waves) emitted from Pile Toe

Pile Depth	Horizontal Distance	Angle	Fv	ks	$Z_{S,P}$	z	E_T	r_T	v_{Sv}
m	m	°	KN		kNs/m^3			m	mm/s
3	10	73	0.80	0.0032	760	2	0.16	10.4	0.42
3	20	81	0.55	0.0032	760	2	0.16	20.2	0.08
3	40	86	0.30	0.0032	760	2	0.16	40.1	0.01
11.5	10	41	1.55	0.0019	2,304	1	0.24	15.2	1.27
11.5	20	60	1.10	0.0019	2,304	1	0.24	23.1	0.39
11.5	40	74	0.70	0.0019	2,304	1	0.24	41.6	0.08
17	10	30	1.75	0.0018	2,592	2	0.53	19.7	2.69
17	20	50	1.30	0.0018	2,592	2	0.53	26.2	1.13
17	40	67	0.90	0.0018	2,592	2	0.53	43.5	0.28
24	10	23	1.85	0.0017	2,736	2	0.56	26.0	2.37
24	20	40	1.50	0.0017	2,736	2	0.56	31.2	1.33
24	40	59	1.10	0.0017	2,736	2	0.56	46.6	0.44

Calculation of Surface Waves due to Spherical Waves

In the theoretical assessment of the vibration propagation from the pile, it was shown that surface waves (R-waves) can be generated when P-waves encounter a free surface (ground surface) at a critical angle, Eq. 33. The critical incidence angle for the different soil layers is given in Table 16 and depends on the ratio of the S-wave and P-wave velocity.

Once the critical distance at the ground surface, r_{crit}, has been calculated, and the vibration amplification factor F_v, is known, the vibration velocity at the critical distance $v_{crit,}$ can be calculated. The results of the calculations for the example pile

are shown in Table 17. The same calculation method was used as for P-waves as described above. It is now necessary to determine the attenuation of ground vibrations due toe geometrical damping and material damping. The absorption coefficient can be estimated from the following relationship, assuming material damping (4 %) and a dominant frequency (15 Hz). An absorption coefficient, α, equal to 0.02 m^{-1} was obtained from Eq. 35. The vibration amplitude, A_2, at distance, R_2, can now be readily calculated from Eq. 34. For surface waves, with an exponent, n, equal to 0.5, the vertical vibration velocities at 10, 20 and 40 m can be calculated, as presented in Table 17.

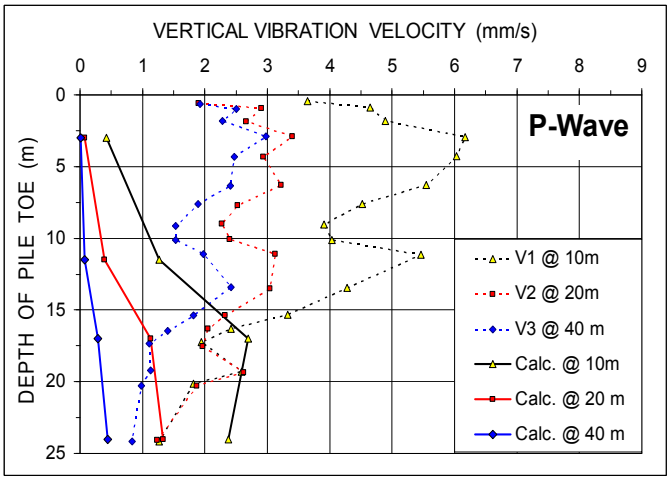

Fig. 26. Measured vertical vibration velocities (dashed lines) and calculated (solid lines) spherical waves (P-waves) emitted from pile toe at 10, 20, and 40 m distance from the pile. Note, P-waves are emitted from the pile toe and do not dominate the measured vibration until the pile toe encounters toe resistance (below about 17 m depth).

Table 16. Determination of critical distance at ground surface at which surface waves are generated. Also shown is the corresponding amplification factor, F_V

	c_P	c_S	H_{crit}	r_{crit}	F_v
Sand fill	400	200	30	1.73	1.7
Clay	1,450	125	5	2.47	2.00
Sandy gravel	1,450	300	12	3.20	1.85
Glacial till	1,450	500	20	5.01	1.65

The calculated vertical vibration velocities according to Table 17 are shown in Fig. 27, together with the measured vibration velocities at corresponding pile penetration depths and distances.

Table 17. Calculation of Surface Waves (R-waves) emitted from pile toe at critical distance

Pile toe m	k_s	$z_{S,P}$ kNs/m^3	z	E_T	v_{crit} mm/s	v10 mm/s	v20 mm/s	v40 mm/s
3	0.0032	760	2	0.16	8.09	4.18	2.42	1.15
11.5	0.0019	2304	1	0.24	2.76	3.1	1.79	0.85
17	0.0018	2592	2	0.26	1.85	2.81	1.63	0.77
24	0.0017	2736	2	0.28	1.19	2.49	1.44	0.68

Fig. 27 shows a good correlation between calculated and actually measured vibration velocities. However, the vibration amplitudes in the upper soil layers are somewhat higher than calculated. This may be due to a higher soil resistance (P and S-wave velocities) than assumed. Moreover, several factors, which can influence ground vibrations, have not been considered, such as superposition of vibrations from different sources (although they occur at different vibration frequencies). An additional possible aspect is that vibration amplification occurs due to resonance effects in the upper soil layer. This effect is not taken into account in the present analysis. In spite of the many simplified assumptions, the model appears to capture the main factors influencing the generation of surface waves, which are caused by emission of vibrations at the pile toe.

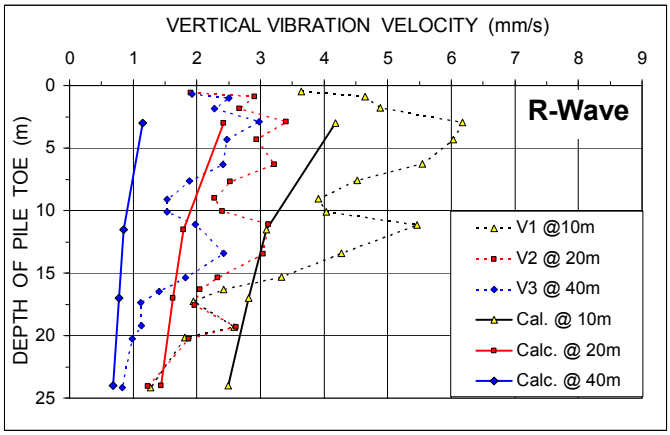

Fig. 27. Vertical vibration velocities (dashed lines) measured at 10, 20, and 40 m distance from the pile and calculated (solid lines) velocities caused by surface waves (R-waves) emitted from pile toe and refracted at the surface.

Calculation of Cylindrical Waves Emitted Along Pile Shaft

Similar to the P-wave emitted from the pile toe, the dynamic resistance along the pile shaft can also be a source of ground vibrations, emitted when the pile shaft moves relative to the soil. Therefore, during the driving through the overburden before the pile toe encounters significant resistance to the penetration, the emitted vibration waves are expected to be cylindrical waves. Vibration attenuation is similar to that of surface waves, but the source and emission pattern are fundamentally different. When the stress wave moves down

the pile, only the part of the pile which corresponds to the wave length of the propagating wave will emit vibrations to the surrounding soil. To calculate the transfer of cylindrical waves along the pile shaft, the wave length, L^W, of the wave propagating in the pile is first calculated from Eq. 14. Then, the vibration efficacy factor E_S that defines the vibrations transferred from the shaft is calculated according to Eq. 19. Note that the shear wave velocity reduction factor R_C is chosen considering the resistance developing along the pile shaft during the driving, as indicated from the penetration resistance (Fig. 16). The variation of the vibration velocity in the horizontal direction from the pile shaft can now be determined from Eq. 37.

An important aspect, which needs to be taken into account, is the effect of soil remolding along the pile shaft, using the empirical R_R-coefficient. In the case of shaft resistance, the value is in most soils lower than unity and can for concrete piles be assumed to be approximately 0.5 (in contrast to toe resistance, where the value can be larger or smaller than unity, depending on soil type). It should also be pointed out that when driving a pile group at close spacing, the lateral earth stress can increase significantly and increase the shaft resistance. The calculation of v_C is summarized in Table 18.

Table 18. Calculation of cylindrical waves (C-waves) emitted along the pile shaft

Emb. depth m	f Hz	k m	z	R_c	L^P m	L_{eff}/b	E_S	k_c	r_c m	v_C mm/s
3.0	15	13	0.5	0.25	3.00	9.85	0.19	0.0020	10	2.3
3.0	15	13	0.5	0.25	3.00	9.85	0.19	0.0020	20	1.7
3.0	15	13	0.5	0.25	3.00	9.85	0.19	0.0020	40	1.2
11.5	13	10	0.5	0.30	4.87	15.97	0.2	0.0021	10	2.4
11.5	13	10	0.5	0.30	4.87	15.97	0.2	0.0021	20	1.7
11.5	13	10	0.5	0.30	4.87	15.97	0.2	0.0021	40	1.2
17.0	15	20	0.5	0.30	4.87	15.97	0.53	0.0013	10	4.3
17.0	15	20	0.5	0.30	4.87	15.97	0.53	0.0013	20	3.0
17.0	15	20	0.5	0.30	4.87	15.97	0.53	0.0013	40	2.1
24.0	15	33	0.5	0.35	4.87	15.97	1	0.0010	10	6.1
24.0	15	33	0.5	0.35	4.87	15.97	1	0.0010	20	4.3
24.0	15	33	0.5	0.35	4.87	15.97	1	0.0010	40	3.0

The calculated cylindrical waves according to Table 18 are shown in Fig. 28 and compared with the measured ground vibrations.

Considering the simplified analysis, the agreement shown in Fig. 28 between calculated and measured vibrations is very good during the driving through the overburden above about 15 m depth. Note that during the final phase of driving, cylindrical waves are overestimated as the relative displacement between the pile shaft and the surrounding soil will be small. Therefore, vibration velocities calculated for the last about 8 m of driving are not representative. However, they are included in Fig. 28 to illustrate the point.

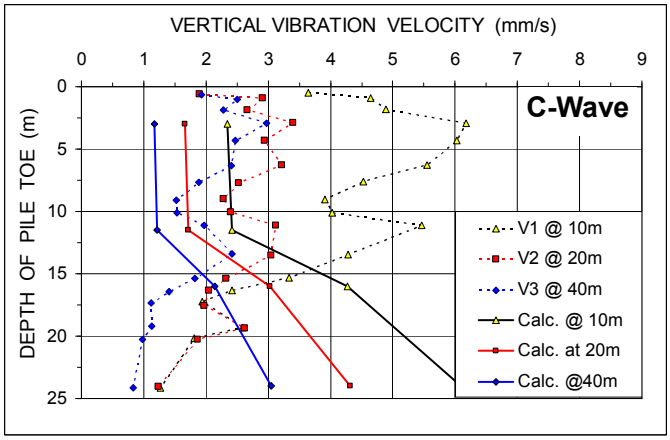

Fig. 28. Measured vertical vibration velocities (dashed lines) and calculated (solid lines) spherical waves (C-waves) emitted from pile toe at 10, 20, and 40 m distance from the pile. Note, cylindrical waves are emitted from the pile shaft and cease to dominate the measured vibration when the pile toe encounters toe resistance (below about 17 m depth).

Comparison of Calculated and Measured Vibrations

In Fig. 29, the vertical vibration velocities determined according to the theoretical approach presented in this paper (for four different depths) are compared with measured vertical vibrations. The theoretical model agrees very well the variation of vibration velocities with distance and envelopes the measured values. However, as has been pointed out in connection with the discussion of Fig. 28 above, vibrations caused by the cylindrical waves in the sandy gravel and glacial till (where pile penetration was small) should be disregarded.

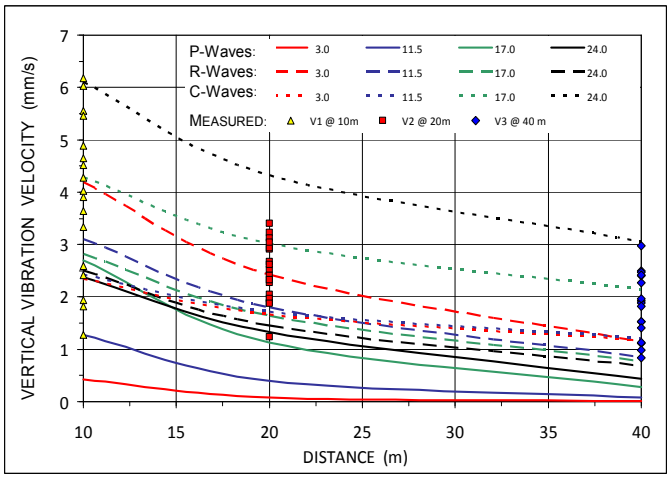

Fig. 29. Comparison of measured and calculated vertical vibration velocities as function of distance for different pile penetration depths for spherical, surface and cylindrical waves, respectively.

Calculation Based on Energy Concept

For comparison, the empirical relationship given in Eq. 3 and shown in Fig. 4 has been used to calculate vibration velocities for the case history. Figure 30 presents the calculated ground vibrations at the horizontal distances from the pile of the three sensor locations for different penetration depths, when assuming a k-value, equal to 0.75 and a nominal energy, W_0, equal to 1,600 J (mass of 4,000 kg and height-of-fall of 0.4 m). Similar to Fig. 26 to 29, the measured vibration velocities are also plotted in the figure. As can be seen, the vibration velocities calculated from the energy concept underestimate the actual velocities considerably. It should also be noted that if only the horizontal distance from the pile location at the ground surface would have been used in Eq. 3, the calculated values shown in Fig. 30 would correspond to those at zero pile penetration depth—agreeing very poorly with the actually measured vibration velocities.

Risk of Damage to Buildings

The main purpose of the pile driving tests at the site was to determine the distance where ground vibrations could be expected to be lower than the limiting value recommended by the Swedish standard. From Eq. 1, the maximum allowable vibration velocity (vertical component) is v_{max} = 10.8 mm/s. According to Fig. 29, at 40 m distance, the maximum vertical vibration velocity would not exceed 4 mm/s and even at 10 m distance the expected maximum value would be below 7 mm/s. The project was completed without any damage to the structures. However, some concern was expressed with regard to environmental considerations (occupants in buildings and vibration-sensitive equipment and installations).

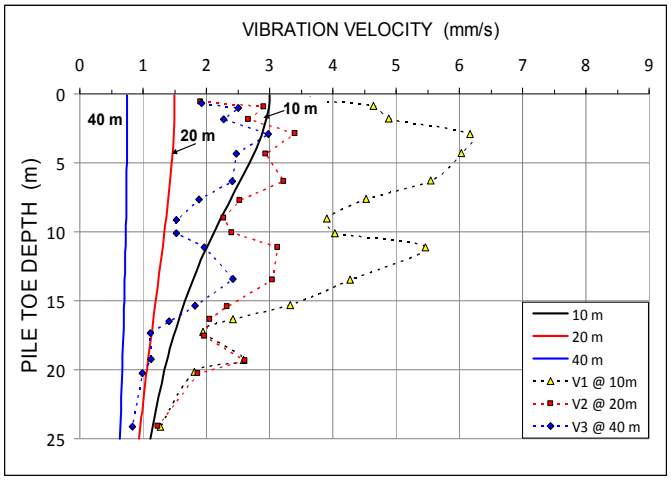

Fig. 30. Ground vibrations calculated according to Eq. 3 at three horizontal distances from the test pile during the driving to the 25 m depth assuming a value of k = 0.75.

CONCLUSIONS AND RECOMMENDATIONS

General Comments

In spite of the wide use of driven piles and sheet piles and the increasing awareness of the public and authorities for environmental problems, little progress has been made in the understanding of ground vibrations caused by impact pile driving. Local codes and standards are available giving advice regarding limiting values of vibration velocity based on local or regional experience, which can be used to assess broadly the risk for damage to nearby structures.

The engineering profession has accepted crude prediction models, based on empirically developed concepts, which do not reflect the key factors controlling the pile driving with regard to vibration emission. This is surprising, because dynamic pile testing and sophisticated analytical methods are commonly used to predict pile drivability and bearing capacity and, as shown, they can be easily adapted to vibration problems.

Requirements Regarding Case History Data

Most case histories describing vibration measurements during pile driving provide insufficient information for a scientific evaluation and interpretation of measurement results. Case histories documenting stress-wave measurements in combination with ground vibration measurements at different distances from the driven pile would offer important information which would facilitate the assessment of how vibration energy is transferred from the pile hammer, along the pile shaft, to the pile toe, and to the surrounding soil layers. However, such information is not available for application to ground vibration problems.

Importance of Pile and Soil Impedance

A fundamental aspect of ground vibrations induced by pile driving is the realization that vibrations are caused by the velocity-dependent soil resistance along the shaft and at the pile toe, which set upper limits to the vibration energy, which can be transferred. Applying the theoretical aspects of pile dynamics, it is possible to estimate with satisfactory accuracy the dynamic forces at the pile head, along the pile shaft and at the pile toe. The guidance provided in this paper combined with basic geotechnical information is in many cases sufficient to assess the dynamic soil properties

The impedance of the pile and of the soil are the single most important parameters for calculating ground vibrations as these govern the transfer and propagation of vibrations in the pile, along the pile-soil interface, and in the surrounding soil.

Limitations of Empirical Methods

Empirical calculation methods used for predicting ground vibrations induced by impact pile driving are based on energy concepts, were initially developed for estimating blasting vibrations. However, the parameters used in the empirical relationships are inconsistent with respect to their units and the different parameters are not defined. For example, the distance to use in assessing the propagation of ground vibrations from the source is not indicated. Consequently, the horizontal distance at the ground surface is often chosen for the predictions, neglecting the fact that in most cases the source of vibrations is either located along the pile shaft and/or at the pile toe.

New Method for Vibration Prediction

This paper presents a new concept that makes it possible to distinguish between different vibration sources (pile shaft and pile toe). It also makes it possible to estimate the maximum vibration transmission, which can occur at the pile-soil interface. The maximum dynamic force imparted to the pile head by the drop hammer can be estimated with sufficient accuracy, provided that the hammer properties (length and impedance) and the hammer height-of-fall are known. The particle velocity in the pile, generated by the propagating stress wave, is an important parameter as this defines the dynamic force. In contrast to present practice, the potential or nominal energy of the pile driving hammer is not relevant for assessing ground vibrations. It is shown that, instead, the hammer properties (impedance and hammer height) as well as the driving method (height-of-drop) govern ground vibration emission.

Three wave types can be caused by pile driving: spherical waves emitted from the pile toe (primarily P-waves), cylindrical wave due to shear along the pile shaft and surface waves which are composed of refracted P- and S-waves, when these encounter the ground surface at a critical angle. It is possible, based on the concepts presented in the paper, to determine the vibration amplitude generated by each of these wave types.

The dynamic (velocity-dependent) soil resistance can be estimated based on the soil impedance at the pile shaft and at the pile toe. Basic concepts developed in pile dynamics can be used to determine these parameters, taking into account that the shear wave velocity of the soil decreases at large strain. Guidelines based on soil plasticity are given which help to estimate the shear wave velocity and reduction factor.

In most soils, the shaft resistance will decrease due to shear strain and remolding. At the pile toe, the soil stiffness and, therefore, the wave velocity can increase due to gradual densification of granular soils, or be reduced as a result of soil disturbance and excess pore water pressure. The paper introduces a vibration transmission factor—vibration efficacy—which adjusts the dynamic force which can be transmitted along the pile-soil interface and thus also the magnitude of ground vibrations.

Vibrations Generated By Pile Driving

Based on elastic theory, the propagation of waves from the pile shaft (cylindrical waves) and at the pile toe (spherical waves) can be analyzed. It can be shown that serious errors are made if empirical concepts are used without taking into account the origin of vibration energy. Closed-form solutions are presented for estimating the parameters needed for the assessment of vibration propagation.

The elastic wave velocities, as determined from seismic field or laboratory measurements must be adjusted, taking into account the effect of strain level. The shear strain level induced by vibrations in soil will be high in the vicinity of the pile and affect the magnitude of wave velocity (the soil will be in the non-elastic range). Thus, also the soil impedance will be affected by strain level.

An important aspect is the fact that vibrations can be amplified or reduced at the ground surface and that the angle of incidence must be taken into consideration. When spherical waves encounter the ground surface at a particular critical angle, the vibrations give rise to waves, propagating along the ground surface — surface waves. Solutions are available to determine the vertical vibration amplitude at the critical distance and to establish the attenuation of the surface wave, taking into account the wave velocity.

The most important advantage of the presented analysis is the improved understanding of how geotechnical and dynamic parameters affect ground vibrations—factors that have been completely neglected in the past. It is believed that, with the increasing availability of stress-wave measurements and ground vibration recordings in the three principal directions and at several distances from the source, the present model can be further refined.

Evaluation of the Case History

A case history providing detailed ground vibration measurements was analyzed, where a concrete pile was driven into a soil deposit consisting of a stiff surface layer on medium stiff clay below which granular soil and glacial till was encountered. This geological formation is rather complex and makes it possible to evaluate the different modes of ground vibration emission from the pile shaft and at the pile toe. Based on detailed vibration measurements and frequency analysis of vibration records, it was possible to identify

different wave types and their likely source of origin (shaft and/or toe) as well as the angle of incidence of waves.

The theoretical concepts presented in this paper were used to calculate ground vibrations during different phases of the driving of a test pile. The calculated vibration values are in good agreement with measured velocities, in spite of the simplifications on which the theory has been based.

Limitations of Proposed Prediction Method

It should be emphasized that the theoretical models presented in this paper are based on assumptions, which limit the validity of vibration predictions. As vibration estimates in most cases must be made prior to field tests, it is necessary to assume a range of input parameters, such as pile driving equipment and installation process, different pile types, and soil profiles. The strength of the proposed model is the possibility to identify the relative importance of different input parameters and their consequence on ground vibrations. No effect of vibration amplification (superposition of different wave types) has been included. Moreover, this simplified model for the transmission of vibrations from the pile to the soil and the propagation of waves (assuming straight rays in each soil layer) and the effect of wave refraction/reflection is expected to be improved, as more case data become available.

Another uncertainty is the superposition of ground vibrations during pile penetration, as the wave propagation process from different depths and sources (at different frequencies) can lead to superposition or canceling of vibration amplitudes.

The frequency content of ground vibrations is of great practical importance. For instance, when the effect of ground vibrations on buildings are considered, the analysis will show whether or not there is a potential for amplified vibration.

However, in spite of the simplifications and uncertainties, the proposed method has shown good correlation with the vibration values measured during the driving of the test pile, and demonstrated that the intensity of ground vibrations is strongly affected by soil resistance along the pile shaft and at the pile toe.

Measures to Reduce Ground Vibrations

When planning piling projects, the design engineer is often required to propose measures to reduce ground vibrations. As has been demonstrated above, the empirical, energy-based model is incorrect and can be misleading. For example, using a hammer with a smaller driving energy (without also a smaller impact force) does not necessarily reduce ground vibrations.

Based on the approach proposed in this paper, the following recommendations are offered for ways to alleviate vibration concerns.

1. Ground vibrations are not directly affected by the driving energy. However, reducing the drop height of the hammer (and thus the impact velocity) will decrease ground vibrations.
2. The length of the pile hammer influences the length of the stress wave (and thus the transfer of vibrations from the pile to the soil). A shorter stress wave will reduce the length of force transfer along the pile shaft, but it can at the same time reduce the ability to drive the pile, in particular for piles with high shaft resistance in sandy soils.
3. One of the most important parameters affecting ground vibrations is pile impedance: ground vibrations increase dramatically with decreasing pile impedance.
4. Ground vibrations will increase with increasing specific soil impedance (z_P at the pile toe and z_S along the pile shaft).
5. Reduction of the contact area between the pile and the soil will decrease ground vibrations.
6. Ground vibrations can be reduced by decreasing soil stiffness (impedance), which can be achieved by different measures, such as pre-boring, water jetting, or changing of pile type.

ACKNOWLEDGEMENTS

The first author wishes to acknowledge the close cooperation and stimulating discussions with Prof. Anders Bodare of the Royal Institute of Technology (KTH) in Stockholm, Sweden. His profound theoretical knowledge of vibration problems and ability to find solutions to challenging problems has been of great importance for the concepts described in this paper. Theses supervised by Dr. Bodare, such as the excellent field measurements presented by Mr. Gunnar Nilsson, have been a valuable source for scientific evaluation. The diligent work and assistance by Mr. Nilsson in making available detailed results of vibration measurements is acknowledged.

The valuable comments by Dr. Martin Jonsson, Dr. Mauricio Ochoa, and David Klingberg in their thorough review of the manuscript are appreciated.

REFERENCES

Attewell, P.B. and Farmer, I.W., [1973]. "Attenuation of ground vibrations from pile driving". Ground Engineering, 6(4) 26 - 29.

Bodare, A., [1997]. "Jord och bergdynamik" (Soil and Rock dynamics). In Swedish. Lecture Handouts, Dept. of Soil and Rock Mechanics, Royal Institute of Technology (KTH), Stockholm, Sweden, 165 p.

Bodare, A., [2005]. "Härledning av förstoringsfaktor vid reflektion av tryckvåg vid fri bergyta" (Derivation of Amplification Factor on Reflection of Pressure Wave at Free Rock Surface). Bilaga 3, SKB Report R-04-06 (Inkapslingsanläggning, Byggbarhetsanalys av bergschakt) by Fredriksson, A. and Johansson S-E., Nitro Consult AB, Niklasson, B. Skanska Teknik AB, December 2005, pp. 109-112.

Brenner, R.P. and Viranuvut, S., [1977], "Measurement and prediction of vibrations generated by drop hammer piling in Bangkok subsoils". Proceedings of the 5th Southeast Asian Conference on Soil Engineering, Bangkok, July 1977, pp. 105-119.

Broms, B.B. and Bredenberg, H., [1982]. "Applications of stress wave theory to pile driving, a State-of-the-Art Report". The 7th Southeast Asian Geotechnical Conference, Hong Kong, 22nd to 26th November 1982, Vol. 2, pp. 195-238.

Clough, R.W. and Penzien, J., [1975]. "Dynamics of structures", McGraw-Hill, 634 p.

Fellenius, B.H., [2006]. "Basics of foundation design". Electronic edition, [www.Fellenius.net], 274 p.

Fellenius, B.H., Riker, R.E., O'Brien, A.J. and Tracy, G.R., [1989]. "Dynamic and static testing in a soil exhibiting setup". American Society of Civil Engineering, Journal of Geotechnical Engineering, 115(7) 984-1001.

Goble, G.G., Tomko, J.J., Rausche, F., and Green, P.M., [1968]. Dynamic studies on the bearing capacity of piles, Vols. 1 and 2, Report No. 31, Division of Solid Mechanics, Structures, and Mechanical Design, Case Western Reserve University.

Goble, G.G., Rausche, F., and Likins, G., [1980]. The analysis of pile driving—a state-of-the-art. Proceedings of the 1st International Seminar of the Application of Stress-Wave Theory to Piles, Stockholm June 1980, Ed. H. Bredenberg, A.A. Balkema Publishers Rotterdam, pp. 131-162.

Goble, G.G., [1995]. "What causes piles to penetrate". Deep Foundations Institute 20th Annual Members Conference and Meeting October 16–18, [1995], Charleston, South Carolina, Proceedings, pp. 95-101.

Heckman, W.S. and Hagerty, D.J., [1978]. "Vibrations associated with pile driving". American Society of Civil Engineering, Journal of the Construction Division, 104 (CO4) 385-394.

Hope, V.S and Hiller, D.M., [2000]. "Prediction of ground borne vibration from percussive piling", Canadian Geotechnical Journal 37(3) 700-711.

Iwanowski, T. and Bodare, A., [1988]. "On soil damping factor used in wave analysis of pile driving". International conference on Application of Stress-wave Theory to Piles, Ed. B.H. Fellenius, Ottawa, May 25-27, 1988, pp. 343-352.

Jedele, L.P., [2005]. "Energy-attenuation relationships from vibrations revisited". GeoFrontiers 2005. Soil dynamics symposium in honor of professor Richard D. Woods. Eds: Stoke, KH II, Anderson, D, Ratje, EM. Austin, Texas, January 24-26, 2005, American Society of Civil Engineers, Geotechnical Special Publication 134, pp. 1467-1480

Martin, D.J., [1980]. "Ground vibrations from impact pile driving during road construction". Transport and Road Research Laboratory, TRRL Supplementary Report 544, 16 p.

Massarsch, K.R., [1992]. "Static and dynamic soil displacements caused by pile driving". Keynote Lecture, Fourth International Conference on the Application of Stress Wave Theory to Piles, the Hague, the Netherlands, September 21-24, 1992, pp. 15 - 24.

Massarsch, K.R., [1995]. "Engineering vibrations and solutions". General Report, Third International Conference on Recent Advances in Geotechnical Earthquake Engineering and Soil Dynamics, April 2-7, 1995, St. Louis, Missouri., Vol. III., pp. 1349-1353.

Massarsch, K.R., [2000]. "Settlements and damage caused by construction-induced vibrations". Proceedings, Intern. Workshop Wave 2000, Bochum, Germany, December 13 - 15, 2000, pp. 299 - 315.

Massarsch, K.R., [2002]. "Ground Vibrations Caused by Soil Compaction". Wave 2002. Proceedings, International Workshop, Okayama, Japan, pp 25 - 37.

Massarsch, K.R., [2004]. "Deformation properties of fine-grained soils from seismic tests". Keynote lecture, International Conference on Site Characterization, ISC'2, September 19-22, 2004, Porto, 133- 146.

Massarsch, K.R., [2005]. “Ground Vibrations Caused by Impact Pile Driving”. Invited Lecture, Proceedings, Environmental Vibrations: Prediction, Monitoring, Mitigation and Evaluation (ISEV 2005). Okayama University, Japan, September 20–22, 2005, Taylor & Francis, pp. 369 - 379.

Massarsch, K.R. and Broms, B.B., [1991]. “Damage Criteria for Small Amplitude Ground Vibrations”, Second International Conference on Recent Advances in Geotechnical Earthquake Engineering and Soil Dynamics, St. Louis, Missouri, March 11-15, 1991, Vol. 2, pp. 1451-1459.

Massarsch, K.R., Westerberg, E., [1995]. ”Frequency-variable vibrators and their application to foundation engineering”. Proceedings, Deep Foundation Institute, 20th Annual Conference, October 16 – 18, 1995, Charleston, South Carolina, pp. 153 – 166.

New, B.M., [1986]. “Ground vibrations caused by civil engineering works”. Transport and Road Research Laboratory, TRRL Research Report 53, 19 p.

Nilsson, G., [1989]. “Markvibrationer vid pålslagning” (Ground vibrations during pile driving). Examensarbete Nr. 3:89. Dept. of Soil and Rock Mechanics, Royal Institute of Technology (KTH). Stockholm, Sweden, 43 p. and Appendix.

Novak, M. and Janes, M., [1989]. “Dynamic and static response of pile groups”. Proceedings of the 12th International Conference on Soil Mechanics and Foundation Engineering, Rio de Janeiro, 13 – 18 August, 1989. Vol. 2, pp. 1175-1178.

Rausche, F., Goble, G.G. and Likins, G.E., [1985]. “Dynamic determination of pile capacity”. American Society of Civil Engineering, Journal of Geotechnical Engineering. 111(GT3) 367-383.

Rausche, F., [2000]. “Pile Driving Equipment. Capabilities, and Properties”. Sixth Conference on the Application of Stress-wave Theory to Piles. Edited by Niyama and Beim, 11-13 September 2000, Sao Paulo, Brazil, pp. 75 – 98.

Richart, F.E., Woods, R.D. and Hall, J.R. [1970]. “*Vibrations of Soils and Foundations*”. Prentice-Hall, Inc., Englewood Cliffs, New Jersey. 414 p.

Swedish Standard. [1999]. “Vibration and shock – Guidance levels and measuring of vibrations in buildings originating from piling, sheet piling, excavating and packing to estimate permitted vibration levels“, (In Swedish). SS 02 52 11. Swedish Institute for Standards, SIS. Stockholm 1999, 7 p.

Selby, A.R., [1991]. “Ground vibrations caused by pile installation”. Proceedings of the 4th International Conference on Piling and Deep Foundations, Stresa, Italy, April 7–12, 1991, pp 497–502.

Smith, E.A.L., [1960]. “Pile driving analysis by the wave equation”. Journal of the Soil Mechanics and Foundation Engineering Division, Proceedings ASCE 86(SM4) 35–61.

Wiss, J.F., [1981]. “Construction vibrations. State of the Art”. American Society of Civil Engineering, Journal of Geotechnical Engineeringl 107(GT2) 167-181.

Woods R.D. and Jedele, L.P., [1985]. “Energy attenuation relationships from construction vibrations”. Proceedings, Proceedings of a Symposium sponsored by the Geotechnical Engineering Division in conjunction with the American Society of Civil Engineering, Convention in Detroit, Michigan. October 22, 1985, pp. 229-246.

NOTATIONS

A = wave front area
A^P = pile cross section area
A_1 = vibration amplitude at distance R_1 from source
A_2 = vibration amplitude at distance R_2 from source

b^P = pile diameter

c = wave propagation velocity
c^H = velocity of stress wave in hammer
c^P = velocity of stress wave in pile
c_C = velocity of cylindrical wave (C-wave) in the soil
c_P = velocity of stress wave (P-wave) in the soil
c_R = velocity of surface wave (R-wave) in the soil approximately equal to shear wave velocity
c_S = velocity of shear-wave (S-wave) in the soil

D = pile embedment depth
D = distance from source (feet)
D_M = material damping in soil

E^P = modulus of elasticity of pile material
E = energy input at source (in foot-pounds) or explosive charge weight per delay (pounds)
E_S = vibration transmission efficacy along pile shaft
E_T = vibration transmission efficacy at pile toe

f = vibration frequency

F_b = Building Factor
F_h = amplification factor horizontal direction
F^H = hammer efficiency factor (Table 7)
F_i = force in pile
F_v = amplification factor vertical direction
F_m = Material Factor
F_g = Foundation Factor

g = acceleration of earth gravity.

h = hammer-height-of-fall

J_c = dimensionless damping factor

k = wave number
k = an empirical vibration factor, a function of impedance (m2/s√J)
k_c = factor for spherical waves given (Table 5)
k_S = factor for spherical waves (Table 5)

K = intercept value of vibration amplitude at $D/\sqrt{E} = 1$ (ft/lb)$^{1/2}$), (inch)

L^H = length of hammer
L^W = length of stress-wave in pile

M^H = mass of hammer (ram)

n = slope or attenuation rate

r = distance from pile (m)
r_{crit} = critical distance from pile at ground surface at which surface waves are generated
r_C = horizontal distance from the pile shaft
r_r = radial distance to the pile toe

R_1 = distance of vibration amplitude A_1
R_2 = distance of vibration amplitude A_2
R_C = reduction factor of shear wave velocity
R_R = reduction factor for remolding
R_S = dynamic soil resistance along the pile shaft
R_T = dynamic portion of the driving resistance at the pile toe

s = ratio of sinus for angles of incidence of the *P*-wave and the *S*-wave
S^P = contact area between the pile shaft and soil

t = duration of impact (i.e., duration of contact between hammer and pile head)

v = vibration velocity
v = peak particle velocity
v = guidance level (vertical component) of critical vibration velocity Swedish Standard
v^H = particle velocity of wave reflected backup the hammer (ram)
v^P = particle velocity (physical velocity) of pile
v_0 = vibration velocity based on soil types — Swedish Standard.
v_0 = particle velocity of the ram at impact
v_v = vertical component of vibration velocity

W = energy input at source (J)
W_e = strain energy
W_k = kinetic energy
W_0 = potential energy of pile hammer

x = distance (m)

Z^H = impedance of hammer (ram)
Z^P = impedance of pile
Z_P = soil impedance for P-waves, at the pile toe
Z_S = soil impedance
z^P = specific impedance of pile
z_P = specific soil impedance for P-waves, (at the pile toe)
z_S = specific soil impedance for shear waves, (at pile shaft)

α = absorption coefficient

λ = wave length

ρ = total density of soil
ρ = material density of soil

ρ^P = density of pile material

ρ_{soi} = total (bulk) soil density
Θ = angle of incidence of spherical wave at ground surface (to the vertical)
Θ_{crit} = critical angle of incidence (from origin of surface waves)

APPENDIX A.
THEORETICAL ASSESSMENT OF ENERGY TRANSMISSION

The empirical approach expressed in Eqs. 2 and 3 is unsatisfactory as it does not consider important aspects, such as the location of energy source (on, near or below the ground surface), material properties, and type of wave propagation. However, if assessing the transmission of vibration energy from an energy source in an elastic medium, it is possible to consider these aspects (Clough and Penzien, 1975).

A.1 Energy in Elastic Medium

In a conservative system the total energy, W_0, is constant and the differential equation of motion can be established by the principle of conservation of energy. The kinetic energy, W_k, is stored in the mass by virtue of its velocity, whereas the potential energy is stored in the form of strain energy in elastic deformation (or work done), W_e,. As the total energy is constant, its rate of change is zero (the sum of the elastic and the kinetic energy).

Eq. (A1) $$W_0 = W_e(t) + W_k(t) = \text{constant}$$

Energy density (energy per volume, J/m^3) can be used to describe energy transmission into an elastic medium.

The energy density, W, is represented by

Eq. (A2) $$W = 0.5 \rho v^2$$

where W = energy density (J/m^3)
ρ = material density (kg/m^3)
v = particle velocity (m/s)

The energy can be potential (positional), W_e, or kinetic, W_k. When the particle velocity, v, is zero, the kinetic energy is zero and all energy has been stored as the elastic strain energy. In contrast, when the displacement is zero, the velocity and kinetic energy are at maximum, and all the elastic strain energy has been released. The total energy, W_0, is therefore limited to:

Eq. (A3) $$W_0 = W_e(t) + W_k(t) = 0.5 \rho \, v^2(t)$$

where W_0 = total energy density (J/m^3)
W_e = potential energy density (J/m^3)
W_k = kinetic energy density (J/m^3)
ρ = material density (kg/m^3)
v = particle velocity (m/s)

A.2 Energy Transmission

The energy transmitted into an elastic medium can now be determined, assuming sinusoidal motion as a function of Time t.

Eq. (A4) $$v = v_0 \sin(kx - \omega t)$$

where v_0 = particle velocity (m/s)
ω = circular frequency, $2\pi f$
f = frequency of vibration
x = distance (m)
k = wave number

The wave number, k, is expressed in Eq. A5.

Eq. (A5) $$k = \frac{2\pi}{\lambda}$$

where λ = wave length (m)

The wave length λ is obtained from Eq. A6.

Eq. (A6) $$\lambda = \frac{c}{f}$$

where λ = wave length
c = is the wave propagation velocity
f = frequency

The energy contained in one wave length, λ, is obtained from Eq. A7.

Eq. (A7) $$W = \rho \, v_0^2 A \int_0^{\lambda} \sin^2 kx \, dx$$

where W = energy density (J/m^3)
ρ = material density (kg/m^3)
v_0 = initial particle velocity (m/s)
A = area of the wave front
k = wave number (Eq. 8)
x = pile penetration (m)

By integration of Eq. A7 to yield Eq. A8, the solution of the total energy density is obtained.

Eq. (A8) $$W = 0.5 \rho v_0^2 \, A \lambda$$

The maximum vibration energy can now readily be calculated for different types of waves (P-waves, S-waves or R-waves). It is possible to determine quantitatively the k-value (Eqs. A5 and A6) for different wave types, taking into account several important factors, such as wave length and material properties

A.3 Spherical Wave

The energy density, W_1, at the distance, r_1, of an expanding wave front of a spherical wave (compression or shear wave) in an infinite elastic medium is expressed in Eq. 12. If the energy contained by the body wave at the source is W_0, then, the energy density, W_1, at the distance, r_1, with a wave front area, A, is expressed in Eq. A9.

Eq. (A9) $$W_0 = W_1 = 0.5(\rho v_1^2 \lambda)(4\pi r_1^2)$$

where W_0 = energy of wave at source
W_1 = energy of wave at distance, r_1, from source
ρ = material density (kg/m^3)
v_0 = particle velocity at distance, r_1 (m/s)
λ = wave length (m)
A = wave front area

The wave front area, A, is expressed in Eq. A10.

Eq. (A10) $$A = 4\pi r_1^2$$

Solving Eq. 12 for v, Eq. A11 is obtained.

Eq. (A11) $$v_1 = \frac{1}{(2\pi\rho\lambda)^{0.5}} \frac{(W_0)^{0.5}}{r_1}$$

A coefficient, k_S, can now be defined according to Eq. A12.

Eq. (A12) $$k_S = \frac{1}{(2\pi\rho\lambda)^{0.5}}$$

The coefficient k_S has the units (m^2/kg)$^{0.5}$. Combining Eqs. A11 and A12, yields Eq. A13.

Eq. (A13) $$v_1 = k_S \frac{(W_0)^{0.5}}{r_1}$$

It is convenient to transform Eq. A11 into Eq. A14.

Eq. (A14) $$v_1 = \frac{1}{(2\pi\rho\lambda)^{0.5}} \left[\frac{r_1}{(W_0)^{0.5}} \right]^{-1}$$

A.4 Rayleigh Wave

The energy density, W_1, at the distance, r_1, of an expanding wave front of a wave traveling along the surface, a Rayleigh wave, in an infinite elastic medium is expressed in Eq. A15. The area of the cylindrical surface is $2\pi r_1 h$.

Eq. (A15) **Error! Bookmark not defined.** $$W_0 = W_1 = 0.5(\rho v_1^2 \lambda)(2\pi r_1 h)$$

Rearranging Eq. A15 for v_1 yields Eq. A16.

Eq. (A16) $$v_1 = \frac{1}{(\pi\rho\lambda h)^{0.5}} \frac{(W_0)^{0.5}}{(r_1)^{0.5}}$$

A coefficient, k_R, is defined as expressed in Eq. A17. The units of k_R are (m/kg)$^{0.5}$. Note that these units are not the same as those of k_S.

Eq. (A17) $$k_R = \frac{1}{(\pi\rho\lambda h)^{0.5}}$$

With the coefficient k_R, taken as a constant, Eq. A17 can be expressed in a simplified form, as shown in Eq. A18.

Eq. (A18) $$v_1 = k_R \frac{(W_0)^{0.5}}{(r_1)^{0.5}}$$

Eq. A18 can be transformed as shown in Eq. A19.

Eq. (A19) $$v_1 = k_R r_1^{0.5} \left(\frac{r_1}{(W_0)^{0.5}} \right)^{-1}$$